Published for SISSA by Springer

Received: *March 12, 2025*
Revised: *October 17, 2025*
Accepted: *November 16, 2025*
Published: *January 7, 2026*

Measurements of the inclusive W and Z boson production cross sections and their ratios in proton-proton collisions at $\sqrt{s} = 13.6$ TeV

The CMS collaboration

E-mail: cms-publication-committee-chair@cern.ch

Abstract: Measurements are presented of the W and Z boson production cross sections in proton-proton collisions at a center-of-mass energy of 13.6 TeV. Data collected in 2022 and corresponding to an integrated luminosity of $5.01\,\mathrm{fb}^{-1}$ with one or two identified muons in the final state are analyzed. The results for the products of total inclusive cross sections and branching fractions for muonic decays of W and Z bosons are $11.93 \pm 0.08\,(\mathrm{syst}) \pm 0.17\,(\mathrm{lumi})\,^{+0.07}_{-0.07}\,(\mathrm{acceptance})\,\mathrm{nb}$ for W^+ boson production, $8.86 \pm 0.06\,(\mathrm{syst}) \pm 0.12\,(\mathrm{lumi})\,^{+0.05}_{-0.06}\,(\mathrm{acceptance})\,\mathrm{nb}$ for W^- boson production, and $2.021 \pm 0.009\,(\mathrm{syst}) \pm 0.028\,(\mathrm{lumi})\,^{+0.011}_{-0.013}\,(\mathrm{acceptance})\,\mathrm{nb}$ for the Z boson production in the dimuon mass range of 60–120 GeV, all with negligible statistical uncertainties. Furthermore, the corresponding fiducial cross sections, as well as cross section ratios for both fiducial and total phase space, are provided. The ratios include charge-separated results for W boson production (W^+ and W^-) and the sum of the two contributions ($\mathrm{W}^\pm$), each relative to the measured Z boson production cross section. Additionally, the ratio of the measured cross sections for W^+ and W^- boson production is reported. All measurements are in agreement with theoretical predictions, calculated at next-to-next-to-leading order accuracy in quantum chromodynamics.

Keywords: Hadron-Hadron Scattering, Vector Boson Production

ArXiv ePrint: 2503.09742

https://doi.org/10.1007/JHEP01(2026)047

JHEP01(2026)047

Contents

1 Introduction

The massive W and Z bosons are fundamental components of the electroweak (EWK) sector of the standard model (SM) of elementary particle physics. The precise determination of their production cross sections in proton-proton (pp) collisions at the CERN LHC is important for probing theoretical predictions, particularly in high orders of perturbative quantum chromodynamics (QCD). Measurements of these cross sections and other parameters of the SM are important in the search for unknown physics beyond the SM, where the productions of W and Z bosons are background processes. This is also relevant when exploring new energy regimes by increasing the center-of-mass energy of the collider.

This article describes measurements of the inclusive total and fiducial W and Z boson production cross sections, as well as their ratios, at $\sqrt{s} = 13.6\,\text{TeV}$. Previous analyses by the ATLAS, CMS, and LHCb Collaborations have reported results at $\sqrt{s} = 2.76$, 5.02, 7, 8, 13, and 13.6 TeV [1–16]. The size of the analyzed data set corresponds to an integrated luminosity of $5.01 \pm 0.07\,\text{fb}^{-1}$, collected when the LHC began to collide protons at the unprecedented center-of-mass energy of 13.6 TeV in 2022. Despite the statistical limitations introduced by the focus on muonic final states, and the relatively small size of this data set collected, the precision of the cross section results exceeds that of previous measurements, which can be attributed to a more precise determination of the integrated luminosity.

JHEP01(2026)047

Events with one or two identified muons in the final state are analyzed. The Z/γ^* Drell-Yan process is measured in the $Z/\gamma^* \to \mu^+\mu^-$ channel for events with an invariant mass of the dimuon pair in the range 60–120 GeV. Since the dominating process in this mass range comes from the production of Z bosons, the Z/γ^* process is referred to as Z boson production in the following. The cross sections for the production of W and Z bosons are measured in fiducial regions, matching the experimentally accessible phase space, and extrapolated to the total cross sections in the full phase space by applying acceptance corrections. In addition, ratios of cross sections are determined with higher precision than the individual cross section results, as several systematic uncertainties — most notably the uncertainty in the integrated luminosity measurement — cancel out when measuring the ratios. Numerical values from all figures are provided in the HEPData record for this analysis [17].

2 The CMS detector

The central feature of the CMS apparatus is a superconducting solenoid of 6 m internal diameter, providing a magnetic field of 3.8 T. Within the solenoid volume are a silicon pixel and strip tracker, a lead tungstate crystal electromagnetic calorimeter (ECAL), and a brass and scintillator hadron calorimeter (HCAL), each composed of a barrel and two endcap sections. Forward calorimeters extend the pseudorapidity coverage provided by the barrel and endcap detectors. Muons are detected in gas-ionization detectors embedded in the steel flux-return yoke outside the solenoid, and measured in both the tracker and the muon system. A more detailed description of the CMS detector, together with a definition of the coordinate system used and the relevant kinematic variables, is reported in refs. [18, 19].

Events of interest are selected using a two-tiered trigger system. The first level (L1), composed of custom hardware processors, uses information from the calorimeters and muon detectors to select events at a rate of around 100 kHz within a fixed latency of about 4 μs [20]. The second level, known as the high-level trigger (HLT), consists of a farm of processors running a version of the full event reconstruction software optimized for fast processing, and reduces the event rate to around 5 kHz before data storage [21, 22].

The particle-flow (PF) algorithm [23] reconstructs and identifies each particle in an event, with an optimized combination of information from the various elements of the CMS detector. The reconstructed vertex with the largest value of summed transverse momentum squared p_T^2 of physics objects is defined as the primary pp interaction vertex (PV) [24]. The energy of photons is obtained from the ECAL measurement. The energy of electrons is determined from a combination of the electron momentum at the PV as determined by the tracker, the energy of the corresponding ECAL cluster, and the energy sum of all bremsstrahlung photons spatially compatible with originating from the electron track. The energy of muons is obtained from the curvature of the corresponding track. The energy of charged hadrons is determined from a combination of their momentum measured in the tracker and the matching ECAL and HCAL energy deposits, corrected for the response function of the calorimeters to hadronic showers. Finally, the energy of neutral hadrons is obtained from the corresponding corrected ECAL and HCAL energies.

The missing transverse momentum vector $\vec{p}_T^{\text{miss}}$ is computed as the negative vector sum of the transverse momenta of all the PF candidates in an event from the PV, and its magnitude is denoted as p_T^{miss} [25]. The $\vec{p}_T^{miss}$ is modified to account for corrections to the energy scale of the reconstructed jets in the event.

3 Data and Monte Carlo simulation

This analysis uses data collected with the CMS detector during part of the 2022 LHC run at a 13.6 TeV center-of-mass energy. Events are selected based on the presence, at the HLT level, of at least one isolated muon with a transverse momentum $p_T > 24$ GeV and a pseudorapidity $|\eta| < 2.4$.

The signal samples for modeling the W and Z boson production are generated in a Monte Carlo (MC) simulation using MadGraph5_amc@nlo version 2.9.9 [26] at next-to-leading order (NLO) in perturbative QCD with up to two outgoing partons at Born level, where the different jet multiplicities have been merged with the FxFx technique [27]. Background processes with top quarks, i.e., the production of top quark-antiquark pairs ($t\bar{t}$) and the production of single top quarks via the t channel or in association with a W boson, as well as diboson events (WW, WZ, ZZ, collectively referred to as VV) are simulated at NLO using powheg version 2 [28–33]. For single top quark events in the t channel, MadSpin [34] is used to describe the top quark decays. Events with electroweak production of a Z or W boson and two jets are simulated with MadGraph5_amc@nlo version 2.9.13 at leading-order (LO) precision in perturbation theory. The pythia 8.306 package [35] is used for the simulation of parton showering, hadronization, and the underlying event, using tune CP5 [36]. In all generated events, the proton structure is described by the parton distribution functions (PDFs) at next-to-NLO (NNLO) provided by NNPDF 3.1 [37]. For all processes, the detector response is simulated with the Geant4 toolkit [38]. Additional pp interactions within the same or nearby bunch crossings (pileup) are simulated with minimum bias and included in all MC simulation samples.

4 Event selection

The decay of the W boson in the muon channel is characterized by the presence of a prompt, energetic, and isolated muon, and large p_T^{miss} originating from the undetected neutrino. The muonic Z boson decay features two prompt, energetic and isolated muons with opposite electric charges, with an invariant mass of the two muons close to the mass of the Z boson, and no intrinsic p_T^{miss} in the event. In the analysis, only decays into muons are considered, as they can be identified more efficiently and their p_T can be measured more precisely by the CMS detector compared with electrons or tau leptons [39–41]. Electrons and taus still indirectly contribute to selected events in the calculation of the missing transverse momentum. The impact from electrons in jets and hardonically decaying taus on the missing transverse momentum is mitigated through a dedicated hadronic recoil correction explained in section 6. The excellent muon performance has also been demonstrated in the recent measurement of the W boson mass by the CMS experiment [42]. Reconstructed muon candidates are required to satisfy a set of quality criteria corresponding to the "tight" working point of the muon identification [39]. The criteria are based on the number of spatial measurements in the silicon tracker and the muon system, the fit quality of the combined muon track, as well as the transverse impact parameter. These criteria largely suppress nonprompt muons from hadron decays and hadron

JHEP01(2026)047

shower remnants in the muon chambers. In addition, muon candidates must be isolated from other activity in the event. The relative muon isolation is defined as the scalar sum of the p_{T} of all particles reconstructed by the PF algorithm, except for the muon, within a cone of size $\Delta R = 0.4$ around the muon track, with $\Delta R = \sqrt{(\Delta\eta)^2 + (\Delta\phi)^2}$, and divided by the muon p_{T}. The relative isolation of the muon, corrected for pileup contributions, must be smaller than 0.15 for this analysis. In addition, the reconstructed muon candidates must satisfy $p_{\mathrm{T}} > 25\,\mathrm{GeV}$ and $|\eta| < 2.4$, ensuring high efficiency of the muon trigger used to collect the data sample.

The W boson candidate events are required to have exactly one identified muon satisfying the criteria described above. Events with a second muon, identified at the "loose" working point, are rejected, reducing the contamination from Z boson events. Muons passing the loose working point are only required to be reconstructed with the PF algorithm and to be matched to a track in the tracker detector [39]. Although W boson events feature large missing transverse momentum, no requirement on that is made at this stage. Instead, this information is used later on for the signal extraction. The transverse mass m_{T}, defined as

$$m_{\mathrm{T}} = \sqrt{2p_{\mathrm{T}}^{\mu}p_{\mathrm{T}}^{\mathrm{miss}}(1-\cos(\Delta\phi))}, \tag{4.1}$$

with the muon transverse momentum p_{T}^{μ}, and $\Delta\phi$ being the azimuthal opening angle between the muon and the $\vec{p}_{\mathrm{T}}^{\mathrm{miss}}$ direction, is a sensitive kinematic variable in this channel, used to distinguish signal from background contributions.

For the selection of Z boson candidate events, two muons satisfying the above described criteria with opposite electric charges are required. Events with additional muons satisfying these criteria are rejected in order to reduce contributions from diboson productions. The invariant mass of the muon pair $m_{\mu\mu}$ is required to be near the Z boson mass, within the range 60–120 GeV. This requirement reduces the relative contribution of nonresonant Drell-Yan production to the signal.

The aim of the analysis is the measurement of the inclusive cross sections of W and Z boson production, hence no requirements on the presence of accompanying hadronic jets in the event are made.

The fiducial regions for the W and Z boson acceptances are defined in the simulated events by a set of kinematic requirements applied to the final states at the generator level, emulating the event selection criteria applied at the reconstruction level. For the W boson production, the fiducial region is defined by the aforementioned kinematic p_{T} and η requirements on the muon, applied before the emission of final-state radiation (FSR). As opposed to the theoretical definition, the event selection in the fiducial measurements is applied at reconstruction level, where the muons may have undergone FSR effects. The effect on the acceptance is at the level of 2% for W boson production, and at the level of 4% for Z boson production and is corrected to ensure consistency in the comparison to theoretical predictions.

5 Analysis strategy

The product of the fiducial cross section for W and Z boson production and the muonic branching fraction can be expressed in a generalized way as:

$$\sigma_{\mathrm{fid}}\mathcal{B} = \frac{N_{\mathrm{sig}}}{\epsilon L} = \frac{N - N_{\mathrm{bkg}}}{\epsilon L}, \tag{5.1}$$

where $\mathcal{B}$ is the branching fraction for either $\mathrm{W}^+ \to \mu^+\nu$, $\mathrm{W}^- \to \mu^-\bar{\nu}$, or $\mathrm{Z} \to \mu^+\mu^-$, N is the number of observed events, N_{sig} and N_{bkg} are the number of signal and background events, respectively, ϵ is the efficiency of the signal events within the fiducial region satisfying the event selection requirements, and L is the integrated luminosity.

In total, three signal regions are used for the analysis: two single-muon regions (μ^+ and μ^-) and one double-muon region ($\mu^+\mu^-$). In the single-muon regions, the transverse mass m_{T} is used to distinguish the $\mathrm{W}^\pm$ boson signal from background processes, and $m_{\mu\mu}$ is used for that purpose in the double-muon signal region for the Z boson signal. All three distributions are fitted simultaneously by means of a binned maximum likelihood fit.

The results for the product of the cross sections and branching fractions in the full phase space are then calculated by dividing the expression for the fiducial region, which is already aligned with the theoretical definition of the signal, by the kinematic acceptance A of this region:

$$\sigma_{\mathrm{tot}}\mathcal{B} = \frac{\sigma_{\mathrm{fid}}\mathcal{B}}{A}. \tag{5.2}$$

The kinematic acceptance A is derived by calculating the ratio of the theoretically predicted signal cross sections with and without the selection requirements corresponding to the definition of the fiducial region:

$$A = \frac{(\sigma_{\mathrm{fid}}\mathcal{B})_{\mathrm{predicted}}}{(\sigma_{\mathrm{tot}}\mathcal{B})_{\mathrm{predicted}}}. \tag{5.3}$$

For the acceptance in the Z boson region, the total cross section of Z boson production in the mass range 60–120 GeV is calculated without any further requirements on the muons and enters the definition of the acceptance at the denominator. For the calculation of the fiducial cross section, which enters the acceptance at the numerator, the muons must additionally fulfill $p_{\mathrm{T}} > 25\,\mathrm{GeV}$ and $|\eta| < 2.4$, emulating the event selection criteria at the generator level. For the acceptance calculation in the W boson regions, the procedure is repeated analogously with a phase space restriction on the mass of the W boson of $m_{\mathrm{W}} > 20\,\mathrm{GeV}$, which ensures the convergence of the resummation calculations without leading to a visible change in the cross section values. The cross sections are computed numerically at NNLO QCD and next-to-next-to-leading logarithmic (NNLL) q_{T} resummation, where q_{T} is the transverse momentum of the W or Z boson, with the program DYTurbo 1.3.2 [43–46] and the NNPDF 3.1 [37] PDF sets. The following ratios are provided as well:

$$R^{\mathrm{W}^+/\mathrm{Z}} = \frac{\sigma(\mathrm{pp} \to \mathrm{W}^+ + \mathrm{X})\mathcal{B}(\mathrm{W}^+ \to \mu^+\nu)}{\sigma(\mathrm{pp} \to \mathrm{Z} + \mathrm{X})\mathcal{B}(\mathrm{Z} \to \mu^+\mu^-)}, \tag{5.4}$$

$$R^{\mathrm{W}^-/\mathrm{Z}} = \frac{\sigma(\mathrm{pp} \to \mathrm{W}^- + \mathrm{X})\mathcal{B}(\mathrm{W}^- \to \mu^-\bar{\nu})}{\sigma(\mathrm{pp} \to \mathrm{Z} + \mathrm{X})\mathcal{B}(\mathrm{Z} \to \mu^+\mu^-)}, \tag{5.5}$$

$$R^{\mathrm{W}^\pm/\mathrm{Z}} = \frac{\sigma(\mathrm{pp} \to \mathrm{W}^\pm + \mathrm{X})\mathcal{B}(\mathrm{W}^\pm \to \mu^+\nu/\mu^-\bar{\nu})}{\sigma(\mathrm{pp} \to \mathrm{Z} + \mathrm{X})\mathcal{B}(\mathrm{Z} \to \mu^+\mu^-)}, \tag{5.6}$$

$$R^{\mathrm{W}^+/\mathrm{W}^-} = \frac{\sigma(\mathrm{pp} \to \mathrm{W}^+ + \mathrm{X})\mathcal{B}(\mathrm{W}^+ \to \mu^+\nu)}{\sigma(\mathrm{pp} \to \mathrm{W}^- + \mathrm{X})\mathcal{B}(\mathrm{W}^- \to \mu^-\bar{\nu})}, \tag{5.7}$$

where some of the systematic uncertainties, including the uncertainty in the integrated luminosity, cancel out. The NNLO+NNLL predictions for the fiducial and total inclusive

Process	$\sigma_{\text{fid}}\mathcal{B} \pm$ (PDF) $\pm$ (scale) $\pm$ (int) in nb	$\sigma_{\text{tot}}\mathcal{B} \pm$ (PDF) $\pm$ (scale) $\pm$ (int) in nb
W^+	$5.490 \pm 0.040\ ^{+0.025}_{-0.048} \pm 0.007$	$12.06 \pm 0.10\ ^{+0.06}_{-0.13} \pm 0.01$
W^-	$4.222 \pm 0.032\ ^{+0.014}_{-0.045} \pm 0.005$	$8.97 \pm 0.07\ ^{+0.05}_{-0.10} \pm 0.01$
$W^\pm$	$9.710 \pm 0.071\ ^{+0.033}_{-0.093} \pm 0.009$	$21.03 \pm 0.16\ ^{+0.11}_{-0.23} \pm 0.01$
Z	$0.7663 \pm 0.0067\ ^{+0.0031}_{-0.0050} \pm 0.0007$	$2.027 \pm 0.015\ ^{+0.008}_{-0.019} \pm 0.001$

Table 1. Predictions for the product of the fiducial and total inclusive cross sections and branching fractions. The first uncertainty is the PDF uncertainty, the second is the QCD scale uncertainty of the calculation, and the third is the integration uncertainty.

Process	$R_{\text{fid}} \pm$ (PDF) $\pm$ (scale) $\pm$ (int)	$R_{\text{tot}} \pm$ (PDF) $\pm$ (scale) $\pm$ (int)
W^+/Z	$7.158 \pm 0.041\ ^{+0.031}_{-0.016} \pm 0.012$	$5.951 \pm 0.027\ ^{+0.008}_{-0.010} \pm 0.004$
W^-/Z	$5.508 \pm 0.030\ ^{+0.003}_{-0.025} \pm 0.009$	$4.424 \pm 0.016\ ^{+0.005}_{-0.006} \pm 0.004$
$W^\pm/Z$	$12.666 \pm 0.069\ ^{+0.034}_{-0.038} \pm 0.016$	$10.375 \pm 0.040\ ^{+0.010}_{-0.016} \pm 0.007$
W^+/W^-	$1.300 \pm 0.003\ ^{+0.005}_{-0.000} \pm 0.002$	$1.345 \pm 0.004\ ^{+0.003}_{-0.001} \pm 0.001$

Table 2. Predictions for the fiducial and total inclusive cross section ratios. The first uncertainty is the PDF uncertainty, the second is the QCD scale uncertainty of the calculation, and the third is the integration uncertainty.

cross sections are shown in table 1, the corresponding cross section ratios in table 2. The PDF uncertainties in the tables are calculated with the NNPDF 3.1 PDF sets. The scale uncertainties, representing missing higher-order contributions in QCD, are evaluated by varying the renormalization and factorization scales. These scales are set to the mass of the dimuon system as the nominal value and varied up and down by a factor of two (omitting the extreme case where both scales are varied in opposite directions). The final scale uncertainty is taken from the maximum deviation. For the cross section ratios, the different scale variations are treated as fully correlated between the cross sections, leading to partial cancellations. The integration uncertainties reflect the uncertainties of the numerical calculation of integrals in DYTurbo. The asymmetric behavior of the scale uncertainties is caused by outliers from different variations of the individual renormalization and factorization scales.

6 Simulation tuning and data calibration

The conditions used for the simulation of the detector are not necessarily identical to the actual conditions during data taking. To mitigate the bias from these differences, several corrections are applied to the simulation. Furthermore, a muon momentum scale calibration as well as a $p_{\mathrm{T}}^{\mathrm{miss}}$ correction are applied to the data.

Differences in the pileup between simulation and data may bias the result of the analysis. To adjust the pileup of simulated events to match the actual conditions during pp collisions, dedicated correction factors are derived from comparing the simulated pileup distribution with the luminosity-based pileup distribution in the detected events. The latter is calculated

JHEP01(2026)047

from the measured instantaneous luminosity in fixed intervals during data taking, and the measured value of the inelastic pp cross section. A weight is calculated to correct the simulated pileup distribution to the one in data. After reweighting the simulated events, the agreement between simulation and data in the distribution of the number of well-reconstructed primary vertices is improved and well within the uncertainties mentioned in section 9.

To account for higher-order effects not present in the MC generators, the simulation for Z boson production is reweighted based on corrections obtained from the difference in the p_{T} distribution of the dimuon system between data and simulation. The same corrections are applied to the simulation of W boson production.

Since the accurate determination of the muon identification, isolation, and reconstruction efficiencies is a crucial part of the cross section measurements, scale factors compensating for the differences between simulation and data are derived for each selection step in bins of η and p_{T} of the muon. A tag-and-probe method [6] is employed for this purpose on the dimuon sample in both data and simulation, with backgrounds subtracted from the data to obtain a pure sample. Tag muons are defined as muons passing the analysis selection requirements as well as being matched to the appropriate trigger object. The exact definition of probe muons depends on the efficiency under study. They are selected among the muons fulfilling the p_{T} and η requirements of the event selection. The efficiency in the tag-and-probe method is defined as the number of probe muons passing a selection criterion divided by the sum of all probe muons before the corresponding selection.

Assuming that the muon efficiency can be factorized as

$$\epsilon_{\mu} = \epsilon_{\mathrm{Trk}}\, \epsilon_{\mathrm{Sta}}\, \epsilon_{\mathrm{ID}}\, \epsilon_{\mathrm{Iso}}\, \epsilon_{\mathrm{Trigger}}, \tag{6.1}$$

the efficiencies are studied one after the other and the definition of the probe muon is given by the passing probe definition of the preceding efficiency stage. The efficiencies under study are the efficiency of the track reconstruction in the inner tracker ϵ_{Trk}, the reconstruction efficiency in the muon detectors (standalone) ϵ_{Sta}, the muon identification efficiency ϵ_{ID}, the muon isolation efficiency ϵ_{Iso}, and the efficiency of the muon trigger $\epsilon_{\mathrm{Trigger}}$. For both data and simulation, the efficiencies are determined in bins of p_{T} and η of the muon and separately for the two electric charges in the case of the trigger efficiency. The charge-dependent difference in trigger efficiency for the collected events is at the per-mille level in the central part of the detector, but increases to the low percent level in the forward region. The scale factors are then obtained as the ratio of the efficiency values in data and simulation and are applied as event weights to the simulated events, depending on the p_{T}, η and the sign of the identified muons in the event.

Further differences between data and simulation arise from the potential occurrence of false assignments of detector information to the preceding bunch crossing [47]. In such cases, the trigger accepts the event in the bunch crossing preceding the actual bunch crossing of interest, and the data of the interesting event are not recorded. To account for this effect, the corresponding muon trigger inefficiency has been measured in data and is applied as a scale factor to simulation. In the central area of the detector, the inefficiency is at the per-mille level, increasing to the percent level in the outer regions.

JHEP01(2026)047

Misalignments and miscalibrations of the detector, uncertainties in the magnetic field of the detector, as well as shortcomings in the simulation of the relevant processes can cause discrepancies in lepton momentum scale and resolution between data and simulation. Muon momentum scale and resolution corrections are derived by comparing the Z boson peak position in the distributions of the invariant mass of the dimuon pair between data and simulation. Correction factors for momentum scale and resolution are derived by fitting the $m_{\mu\mu}$ distributions in multiple bins of muon p_{T} and η. The signal shape is parameterized by convolving a Breit-Wigner function and a double-sided Crystal Ball function [48, 49]. The mean and the width of the Breit-Wigner function are fixed to the known mass and width of the Z boson. The Gaussian part of the double-sided Crystal Ball function is symmetric and models detector effects, while its exponential sides account for further effects, such as radiative tails.

The momentum scale correction factors are given by the ratio of the fitted peak positions of the $m_{\mu\mu}$ distributions in simulation and data, $\langle m_{\mu\mu}^{\mathrm{MC}} \rangle$ and $\langle m_{\mu\mu}^{\mathrm{data}} \rangle$. These factors, typically at the per-mille level, are applied to the p_{T} of muons in data:

$$p_{\mathrm{T}}^{\text{data, corr.}} = p_{\mathrm{T}}^{\text{data}} \frac{\langle m_{\mu\mu}^{\mathrm{MC}} \rangle}{\langle m_{\mu\mu}^{\mathrm{data}} \rangle}. \tag{6.2}$$

The total width of the fitted peak in the $m_{\mu\mu}$ distribution consists of the intrinsic decay width of the Z boson and the additional contribution from the detector resolution, which is smaller in the simulation compared with data. To mitigate this effect, an additional Gaussian smearing is introduced and applied to the simulated samples to match the momentum resolution observed in data. The width of the Gaussian smearing varies, ranging from zero (indicating no smearing is required) up to 1.5%, with an average value of around 0.6%.

In addition, a precise reconstruction of the muon momentum, the accurate reconstruction of the missing transverse momentum of an event is essential for this analysis, as $p_{\mathrm{T}}^{\mathrm{miss}}$ is used through m_{T} to distinguish W boson production from the background from SM events composed uniquely of jets produced through the strong interaction (QCD multijet events). The predictions for $p_{\mathrm{T}}^{\mathrm{miss}}$ rely on the modeling of the W boson recoil and detector effects, which can be difficult to simulate accurately. Possible sources of discrepancy between simulation and data could result from deficiencies in the modeling of the calorimeter response and resolution or from incomplete description of the underlying event, as well as the displacement of the interaction point. An observed modulation of $p_{\mathrm{T}}^{\mathrm{miss}}$ in the azimuthal angle is mitigated using corrections based on the average value of $p_{\mathrm{T}}^{\mathrm{miss}}$ in the x and y direction. This correction is applied to both data and simulation. Further residual discrepancies between data and simulation are addressed through corrections derived from a study of the Z boson recoil. The recoil is decomposed into two components relative to the Z boson momentum: one parallel and one perpendicular to the boson direction. Corrections are then obtained by aligning the cumulative distribution functions of these recoil components between data and simulation in bins of the W and Z boson momentum.

The fully corrected distributions of the leading (highest p_{T}) and trailing (second highest p_{T}) muon transverse momenta, as well as the $p_{\mathrm{T}}^{\mathrm{miss}}$, both in the Z boson signal region, are shown in figure 1.

JHEP01(2026)047

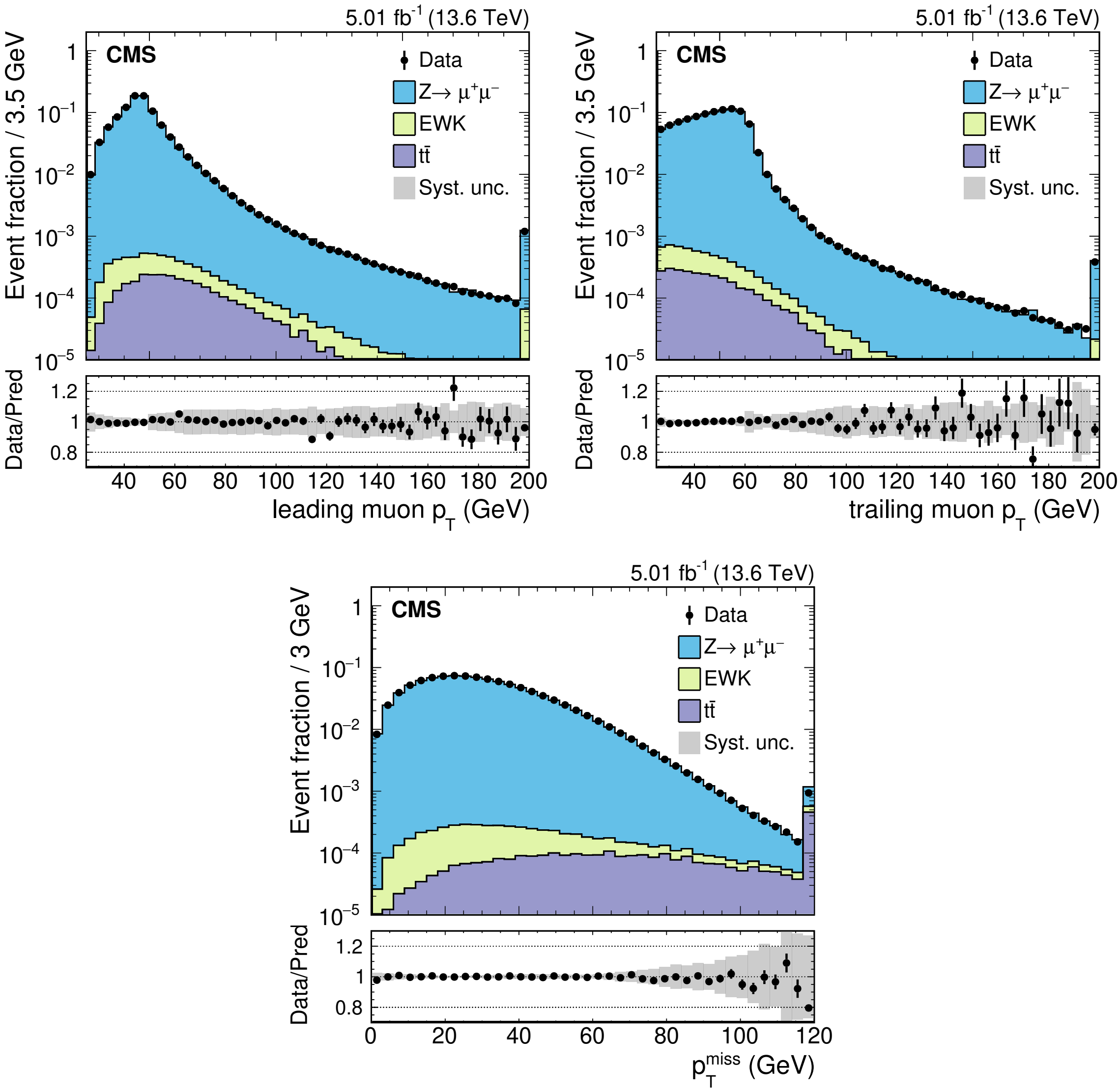

Figure 1. Corrected distributions of the p_T of the leading (upper left) and trailing (upper right) muon, as well as p_T^{miss} (lower) in the Z boson signal region. The distributions of both data and combined simulation in the upper panels are normalized because the scale of the signal sample is extracted later in the fit. The lower panels show the ratio of the normalized data to the normalized prediction. Overflow entries are included in the rightmost bin, respectively. Differences in the shape between data and prediction are fully covered by the systematic uncertainty band. The systematic uncertainties are described in detail in section 9. The vertical uncertainty bars on the data represent the statistical uncertainty.

7 Background modeling

Various background processes must be considered in the analysis, which are grouped into three distinct categories: $t\bar{t}$, EWK, and QCD multijet production. Background categories with prompt muons relevant for this analysis are divided into $t\bar{t}$ and EWK categories, whereas nonprompt muons contribute to the QCD category.

The $t\bar{t}$ category consists of the production of top-quark-antiquark pairs. The production of single top quarks, VV production, the EWK production of a W or Z boson (V) via vector boson fusion in association with two jets (VBF V), and contributions from W or Z bosons decaying into τ leptons, which subsequently decay to muons, are considered in the EWK category. All these background processes are modeled using samples of simulated events. The contribution from W bosons plus hadrons misidentified as a muon in the $(\mu^+\mu^-)$ signal region is negligible.

The third background category, QCD multijet events, comes from SM events composed uniquely of jets produced from the strong interaction. The muon comes from a weak decay within one of the jets or from a jet misidentified as a muon when the jet is not fully absorbed in the HCAL and reaches the muon detectors. This background contribution is only present in the W boson selection, where it is already greatly reduced by the isolation requirement on the muon candidates. However, because of the large production cross section, the remaining QCD multijet events represent the largest background contribution to the single-muon signal regions. Although the normalization of the QCD multijet background is determined in the fit, its shape as a function of m_T is modeled using data events from a QCD-enriched control region. This region is defined by the same event selection requirements as the W boson signal region, with the exception of the muon isolation requirement, which is inverted.

The remaining non-QCD contribution in this QCD-enriched control region is subtracted using simulated samples. The QCD-enriched region is divided into several subsamples, depending on the value of the relative isolation of the muon in the event. In total, 16 subsamples are created in the relative isolation range 0.20–1.00 with a step size of 0.05. The m_T distributions for these subsamples are normalized to the same area, and for each m_T bin, the 16 corresponding values from the different subsamples are fitted to account for the dependence of the m_T distribution shape on the relative isolation of the muon observed in data. The fit is performed using two different fit functions, a linear and a quadratic one. Four fits in different m_T bins are exemplary shown in figure 2. The extrapolation to the signal region (where the muon is isolated) is evaluated at the mean of the isolation distribution created by subtracting the distribution for non-QCD events from the distribution in data for each m_T bin. The template derived from the linear fit function is chosen to be the nominal m_T template and the difference to the template derived from the quadratic fit function is symmetrized and incorporated as a contribution to the QCD template shape uncertainty. Both templates are shown in figure 3. The assumption that the shape of the m_T distribution for QCD multijet events in the QCD-enriched control region is consistent with that in the single-muon signal regions is tested by splitting the control region. Roughly half of the region, with muon relative isolation values between 0.5 and 1.0, is used to derive a QCD m_T template in the other half, with relative isolation values between 0.2 and 0.5. The resulting template in the part of the control region with isolation values between 0.2 and 0.5 is then used to fit the m_T distribution. The resulting post-fit distribution describes the data in the control region with a precision better than one percent.

JHEP01(2026)047

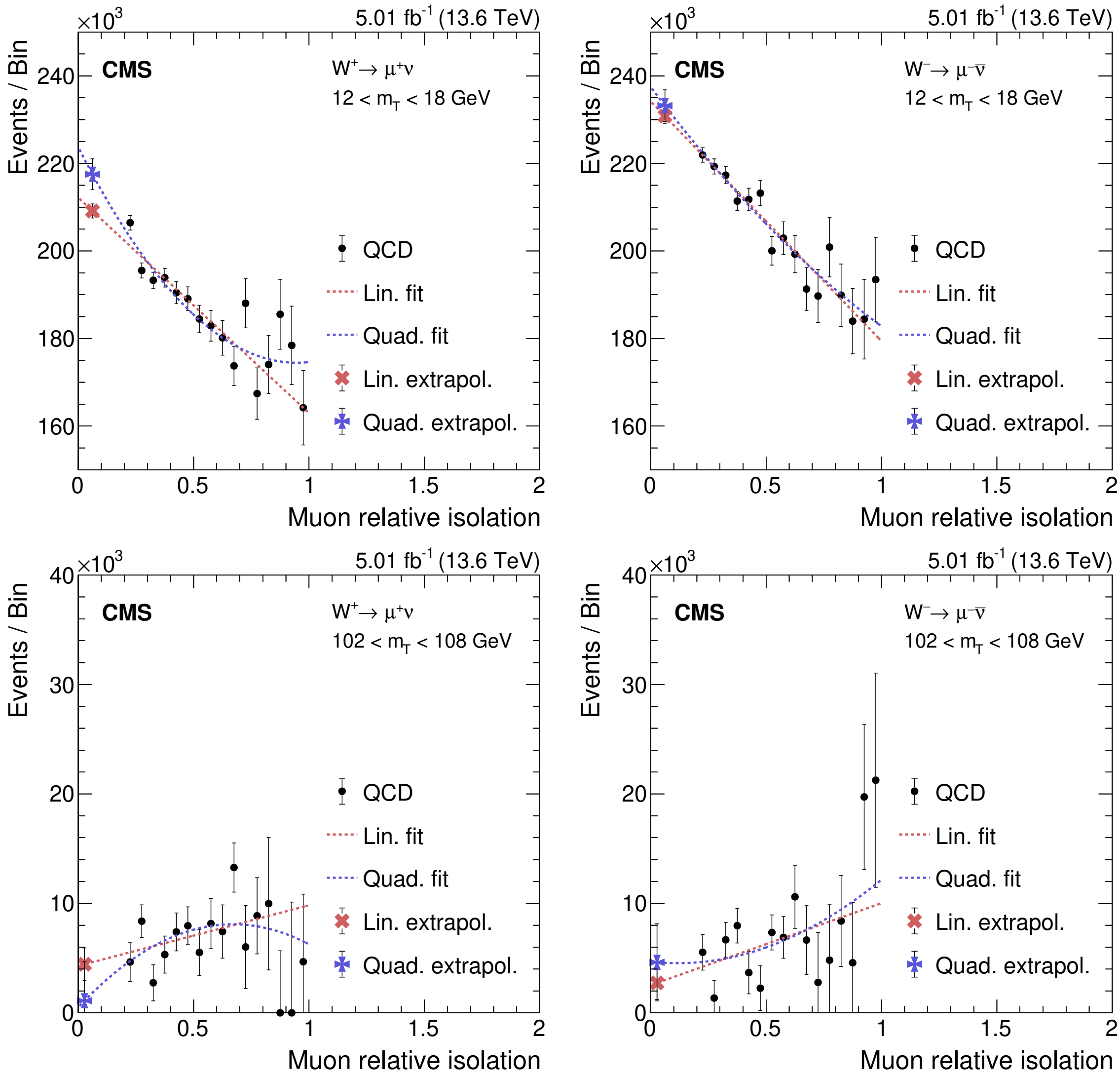

Figure 2. Example figures to illustrate the extrapolation procedure to estimate the QCD multijet background from the QCD-enriched control region. The yield in each bin is obtained by subtracting the simulated non-QCD contributions from the measured data. At high values of the transverse mass, the statistical uncertainty of the QCD yield increases, represented by the vertical uncertainty bars, leaving more freedom for the polynomial fit.

8 Signal extraction

To extract the W and Z boson signal and background yields, a binned maximum likelihood fit is performed simultaneously to the transverse mass m_{T} distributions in the single-muon signal regions and the dimuon invariant mass $m_{\mu\mu}$ distribution in the double-muon signal region. The results are determined using the CMS statistical analysis tool COMBINE [50], which is based on the RooFit [51] and RooStats [52] frameworks.

The m_{T} and $m_{\mu\mu}$ templates are fitted to the observed distributions as the sum of three signal contributions — the W^+, W^-, and Z signals — as well as three distinct background contributions — the $\mathrm{t\bar{t}}$ background, the EWK background, and the background from QCD

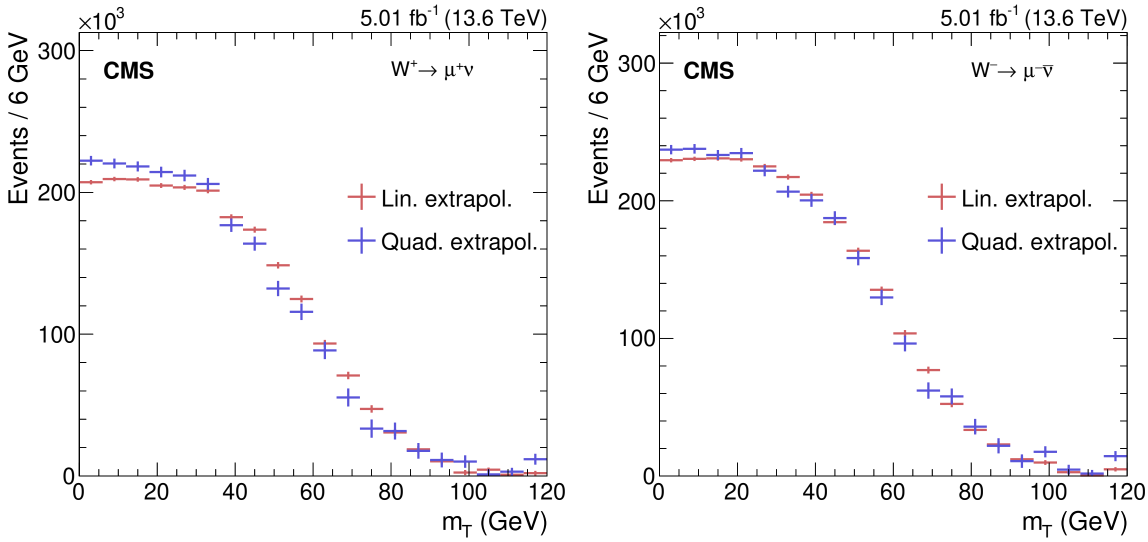

Figure 3. Result of the extrapolated m_{T} distribution for the QCD multijet background in the signal region from the QCD-enriched control region. The template normalization is left freely floating in the fit, as the final normalization is determined in the fit. The vertical uncertainty bars correspond to the extrapolation uncertainty from the fit.

multijet production. The signal and non-QCD background processes are modeled using simulation, with the simulated samples normalized using the theoretically predicted cross sections. The Z boson sample is normalized using the theoretical cross section calculated at NNLO in QCD and NNLL q_{T} resummation with the program DYTurbo and the NNPDF 3.1 PDF sets. The cross sections of top quark-antiquark pair production, W boson production, single top quark production in the tW channel, and diboson production cross sections are taken from ref. [53]. Single top quark production in the t channel has been calculated at NNLO in QCD with the MCFM version 10.1 program [54], and the cross section of the EWK production of a Z boson and two jets is calculated at LO using MadGraph5_aMC@NLO. The pre-fit normalization of the data-driven QCD distributions is taken from the extrapolated templates. The event rates serve as inputs to the maximum likelihood fit and the individual normalization factors of the two QCD templates are finally determined through the fit itself, where they are allowed to vary freely. The kinematic ranges in which the fits are performed are 0–120 GeV for m_{T} and 60–120 GeV for $m_{\mu\mu}$. Systematic uncertainties are included in the maximum likelihood fit as nuisance parameters. The various sources of systematic uncertainty are detailed in the next section, where the individual values correspond to the width of the Gaussian constraint term for the respective nuisance parameter [55].

9 Systematic uncertainties

Several sources of systematic uncertainty influence the results of this measurement. The uncertainty in the muon efficiency scale factors contains statistical and systematic components. The systematic uncertainty component is related to the model dependence of the approach used to extract the numbers of passing and failing probe muons from data. To estimate

JHEP01(2026)047

the impact of this uncertainty source, alternative models for the description of signal and background are used, the p_T requirement on the tag muon is altered, and the mass binning and the fit range are varied. Systematic as well as statistical uncertainty components are also included for the trigger inefficiency. The uncertainty in the muon momentum correction is conservatively considered with 50% of the total correction value. The recoil correction comes with statistical and systematic uncertainty components. The latter is estimated by using alternative fitting models, omitting the background subtraction, and varying the rapidity binning for the determination of the recoil corrections. A 10% uncertainty in the normalization of the backgrounds from simulation is assumed. The model of the QCD multijet process is derived from the experimental data, where the uncertainties in the contamination from non-QCD processes in the QCD-enriched control region and in the choice of extrapolation function, as well as the statistical component, are included. A potential bias in the method used to reweight the pileup distribution in the simulation is evaluated by varying the value of the inelastic pp cross section. The systematic uncertainty of the boson p_T reweighting is considered by taking the difference between the unweighted and the weighted distribution into account. Both pileup and boson p_T reweighting uncertainties are constructed to affect only the shape and not the normalization of the distributions. The finite size of the simulation samples limits the achievable precision of the results, the corresponding systematic uncertainty is modeled by applying bin-by-bin statistical uncertainties in the fit using the Barlow-Beeston "lite" approach [56].

The simulations rely on choices made in the theoretical description of the process. Similar to the reweighting uncertainties, the uncertainties in the theoretical description are constructed to have only a shape but no normalization effect. The uncertainty in the PDFs is estimated by evaluating the set of Hessian uncertainties in the NNPDF 3.1 set, treating each of the 100 variations as an independent nuisance parameter in the measurement. An additional uncertainty in the PDFs is added to account for the choice of the value of the strong coupling at the Z boson mass $\alpha_S(m_Z) = 0.118 \pm 0.002$ at which the PDFs are evaluated. The uncertainties in the renormalization and factorization scales are accounted for by varying these scales up and down by a factor of 2 or 1/2 (omitting the extreme case where both scales are varied in opposite directions). The uncertainty from the choice of $\alpha_S$for the initial- and final-state radiation (ISR, FSR) uncertainty of the parton shower is estimated using up and down variations of the ISR and FSR parton shower scales with a factor of 2.

The dominating source of systematic uncertainty is the uncertainty in the integrated luminosity, which is measured with a precision of 1.4% after a calibration with a method based on van der Meer scans and including systematic effects in the integration of detector rates [57, 58].

The sizes of the systematic uncertainties in percentage of the fit results for the fiducial cross section measurement are summarized in table 3 and for their ratios in table 4. For the W^+/W^- ratio, the leading uncertainties cancel to a large extent, as a result of strong positive correlations between the systematic uncertainties in these two regions. For the W/Z ratios, the magnitude of the leading uncertainties remains comparable to those in the W regions. For the muon efficiency, this follows from the similarity of the muon properties from a W or Z boson decay, resulting in an effective cancellation of the systematic impact of one muon.

JHEP01(2026)047

Uncertainty source	Uncertainty in $\sigma_{\text{fid}}\mathcal{B}$ (in %) for			
	W^+	W^-	$W^\pm$	Z
Muon efficiency	0.28	0.29	0.29	0.40
Finite size of MC samples (bin-by-bin)	0.27	0.27	0.25	0.08
QCD background	0.53	0.49	0.49	0.07
PDF, scales, and parton shower	0.25	0.25	0.25	0.06
Muon momentum correction	0.01	0.02	0.01	0.03
Recoil correction	0.09	0.08	0.08	0.02
EWK background normalization	0.05	0.05	0.05	0.02
Z boson p_{T} correction	0.03	0.04	0.03	0.01
$t\bar{t}$ background normalization	0.01	0.03	0.02	0.01
Pileup	0.01	0.02	<0.01	<0.01
Total	0.68	0.66	0.65	0.42
Integrated luminosity	1.4	1.4	1.4	1.4
Statistical uncertainty	0.03	0.03	0.02	0.06

Table 3. Post-fit uncertainties in percent for the fiducial cross section measurement. For completeness, also the integrated luminosity and statistical uncertainty are given.

Uncertainty source	Uncertainty in R_{fid} (in %) for			
	W^+/Z	W^-/Z	$W^\pm/Z$	W^+/W^-
Muon efficiency	0.27	0.29	0.28	0.02
Finite size of MC samples (bin-by-bin)	0.26	0.26	0.25	0.19
QCD background	0.52	0.47	0.48	0.29
PDF, scales, and parton shower	0.24	0.24	0.24	0.04
Muon momentum correction	0.04	0.05	0.04	0.01
Recoil correction	0.10	0.09	0.09	0.04
EWK background normalization	0.07	0.07	0.07	<0.01
Z boson p_{T} correction	0.04	0.05	0.05	0.01
$t\bar{t}$ background normalization	0.02	0.04	0.03	0.02
Pileup	0.01	0.02	<0.01	0.03
Total	0.68	0.66	0.64	0.38
Statistical uncertainty	0.07	0.07	0.06	0.04

Table 4. Post-fit uncertainties in percent for the fiducial cross section ratio measurement. For completeness, also the statistical uncertainty is given.

Uncertainties with asymmetric uncertainty magnitudes for the different cross sections do not change significantly. Some of the smaller uncertainties are negatively correlated and therefore increase for the cross section ratios, e.g., the uncertainty in the muon momentum resolution correction, which has a strong effect on the dimuon mass shape but a negligible effect on the transverse mass shape, where the resolution is dominated by the missing transverse momentum. In the fit, this strong effect in the dimuon mass shape is buffered through

JHEP01(2026)047

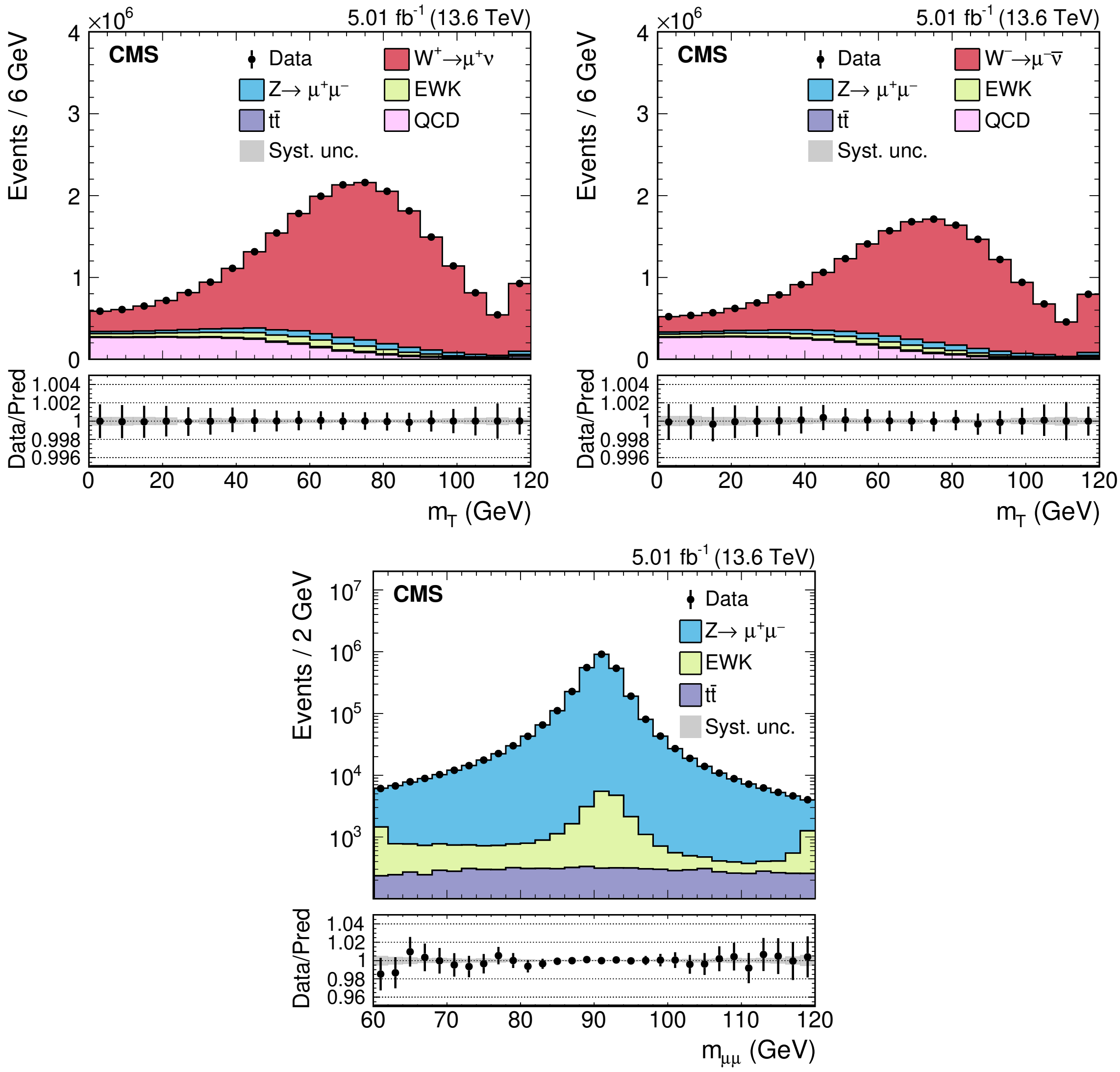

Figure 4. The post-fit distributions of (upper left) $\mu^+\nu_\mu$, (upper right) $\mu^-\bar{\nu}_\mu$, and (lower) $\mu^+\mu^-$ signal regions. The lower panel in each plot shows the ratio of the number of events observed in data to that of the signal and background predictions. Overflow entries are included in the rightmost bin for the two upper plots. The vertical uncertainty bars on the data represent the statistical uncertainty.

variations of further systematic uncertainties, leading to the different behavior in the two regions and therefore resulting in negative correlation.

10 Results

Figure 4 shows the results of the fit to the m_T and $m_{\mu\mu}$ distributions in the single- and double-muon signal regions, respectively. Good agreement between the model, which contains high degrees of freedom for the QCD multijet template, and the data is observed. The expected event yields for the SM expectations of the different processes are shown in table 5 and the observed event yields are shown in table 6.

Process	μ^+ region	μ^- region	$\mu^+\mu^-$ region
$W^\pm$	20 035 607	15 591 566	—
Z	958 372	896 734	2 944 611
EWK:	(989 729)	(801 381)	(27 526)
W ($\to \tau\nu_\tau$)	608 711	498 487	—
Z ($\to \tau\tau$)	119 263	114 194	2 177
W (nonfiducial)	121 304	72 035	—
Z (nonfiducial)	9 000	8 789	16 165
VV	45 062	42 333	6 500
VBF V	21 284	16 522	1 680
Single top quark	65 106	49 021	1 004
$t\bar{t}$	215 409	216 695	9 278

Table 5. Pre-fit event yields in the fiducial region. A dash indicates that the corresponding contribution is found to be negligible in this signal region.

Process	μ^+ region	μ^- region	$\mu^+\mu^-$ region
$W^\pm$	$20\,013\,000 \pm 31\,000$	$15\,665\,000 \pm 22\,000$	—
Z	$966\,700 \pm 2\,300$	$905\,000 \pm 2\,300$	$2\,962\,980 \pm 970$
EWK	$966\,000 \pm 14\,000$	$782\,000 \pm 11\,000$	$26\,560 \pm 460$
$t\bar{t}$	$200\,800 \pm 3\,400$	$202\,100 \pm 3\,400$	$8\,630 \pm 130$
QCD multijet	$2\,973\,000 \pm 33\,000$	$2\,920\,000 \pm 24\,000$	—
Total	$25\,119\,600 \pm 1\,500$	$20\,475\,200 \pm 1\,300$	$2\,998\,160 \pm 850$
Data	25 119 622	20 475 186	2 998 125

Table 6. Post-fit event yields in the fiducial region. The post-fit uncertainties include only statistical and systematic uncertainties, but not the uncertainty in the luminosity. The individual uncertainties in the event yields for a given process are derived by taking the full covariance matrix into account. A dash indicates that the corresponding contribution is found to be negligible in this signal region.

The results for the product of the fiducial and total cross sections of inclusive W^+, W^-, $W^\pm$, and Z boson production and the branching fraction for the muon decay channels are summarized in table 7, along with the corresponding theoretical acceptance predictions. The measured ratios of cross sections and their predicted acceptance values are given in table 8. Theoretical predictions of the product of the cross sections and branching fraction for the muonic decay are computed at NNLO+NNLL QCD accuracy in DYTurbo using the NNPDF 3.1 [37], CT18 [59], and MSHT20 [60] PDF sets. Figure 5 shows comparisons between these predictions and the measured values. The corresponding ratios of the cross sections are shown in figure 6. As the NNPDF 3.1 PDF set is used for the extrapolation of the fiducial result into the total phase space, the corresponding ratio of theoretical to measured values is consistent between the plots for the fiducial and total phase space. For the other PDF sets, however, the ratio is not necessarily the same between the two phase spaces, as the acceptance of the corresponding PDF set and the one of the NNPDF 3.1 set used for the extrapolation of the measured value into the total phase space may differ.

JHEP01(2026)047

Process	$\sigma_{\text{fid}}\mathcal{B} \pm$ (syst) $\pm$(lumi) in nb	Acceptance $\pm$ (PDF) $\pm$ (scale) $\pm$ (int) in %	$\sigma_{\text{tot}}\mathcal{B} \pm$ (syst) $\pm$ (lumi) $\pm$ (acceptance) in nb
W^+	$5.428 \pm 0.037 \pm 0.076$	$45.48 \pm 0.24\,^{+0.11}_{-0.07} \pm 0.07$	$11.93 \pm 0.08 \pm 0.17\,^{+0.07}_{-0.07}$
W^-	$4.167 \pm 0.028 \pm 0.058$	$47.06 \pm 0.22\,^{+0.19}_{-0.10} \pm 0.07$	$8.86 \pm 0.06 \pm 0.12\,^{+0.05}_{-0.06}$
$W^\pm$	$9.60 \pm 0.06 \pm 0.13$	$46.15 \pm 0.22\,^{+0.14}_{-0.08} \pm 0.05$	$20.79 \pm 0.14 \pm 0.29\,^{+0.11}_{-0.12}$
Z	$0.764 \pm 0.003 \pm 0.011$	$37.80 \pm 0.19\,^{+0.14}_{-0.04} \pm 0.04$	$2.021 \pm 0.009 \pm 0.028\,^{+0.011}_{-0.013}$

Table 7. Results for the product of the fiducial and total inclusive cross sections and branching fractions measurements. For the measured values the quoted uncertainty represents the systematic uncertainty, while the statistical uncertainty is negligible. For the acceptance predictions, as explained in section 5, the first uncertainty is the PDF uncertainty, the second is the scale uncertainty, and the third is the integration uncertainty of the calculation.

Process	$R_{\text{fid}} \pm$ (stat) $\pm$ (syst)	Acceptance ratio $\pm$ (PDF) $\pm$ (scale) $\pm$ (int)	$R_{\text{tot}} \pm$ (stat) $\pm$ (syst) $\pm$ (acceptance)
W^+/Z	$7.105 \pm 0.005 \pm 0.048$	$1.203 \pm 0.003\,^{+0.004}_{-0.002} \pm 0.002$	$5.906 \pm 0.004 \pm 0.040\,^{+0.022}_{-0.028}$
W^-/Z	$5.455 \pm 0.004 \pm 0.036$	$1.245 \pm 0.004\,^{+0.001}_{-0.005} \pm 0.002$	$4.382 \pm 0.003 \pm 0.029\,^{+0.023}_{-0.016}$
$W^\pm/Z$	$12.559 \pm 0.008 \pm 0.081$	$1.221 \pm 0.003\,^{+0.003}_{-0.003} \pm 0.002$	$10.288 \pm 0.007 \pm 0.066\,^{+0.037}_{-0.037}$
W^+/W^-	$1.303 \pm 0.001 \pm 0.005$	$0.966 \pm 0.003\,^{+0.003}_{-0.002} \pm 0.002$	$1.348 \pm 0.001 \pm 0.005\,^{+0.006}_{-0.007}$

Table 8. Ratios of the measured product of the fiducial and total inclusive cross sections and branching fractions along with the corresponding acceptance predictions. Since some contributions of the systematic uncertainty, most prominently the luminosity uncertainty, cancel out in the ratios, the statistical component becomes relevant. For the acceptance predictions, as explained in section 5, the first uncertainty is the PDF uncertainty, the second is the scale uncertainty, and the third is the integration uncertainty of the calculation.

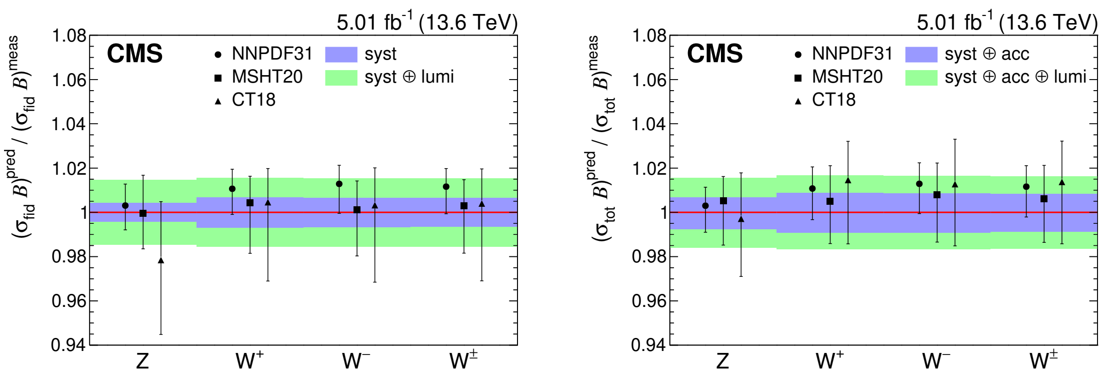

Figure 5. Comparison of measured product of fiducial (left) and total (right) cross sections and branching fractions with different theoretical predictions at NNLO+NNLL QCD accuracy. The vertical uncertainty bars on the markers represent the total uncertainty of the theoretical prediction.

A comparison of measured products of total cross section and branching fraction at other center-of-mass energies with the corresponding theoretical prediction is shown in figure 7.

JHEP01(2026)047

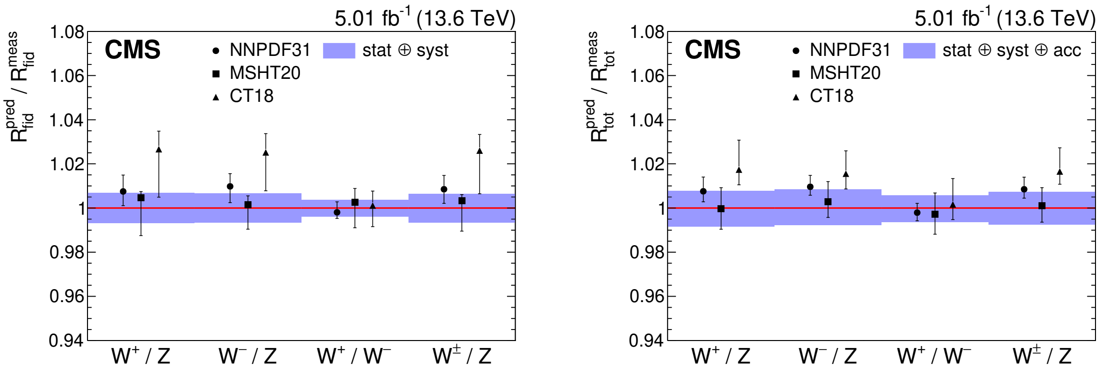

Figure 6. Comparison of measured fiducial (left) and total (right) ratios with different theoretical predictions at NNLO+NNLL QCD accuracy. The vertical uncertainty bars on the markers represent the total uncertainty of the theoretical prediction.

11 Summary

Measurements of fiducial and total inclusive W and Z boson production cross sections multiplied by the $W \to \mu\nu_\mu$ and $Z \to \mu^+\mu^-$ branching fractions, respectively, in proton-proton collisions at 13.6 TeV are presented. Muon final states are studied in data samples collected with the CMS detector corresponding to an integrated luminosity of $5.01 \pm 0.07\,\mathrm{fb}^{-1}$. The measured Z boson cross section is defined as the inclusive Drell-Yan Z/γ^* production of muon pairs in the invariant mass range of 60–120 GeV, where the production of a Z boson is the dominant contribution. The results for the product of total inclusive cross sections and branching fractions are:

$$\begin{aligned}
\sigma(\mathrm{pp} \to \mathrm{W}^+{+}\mathrm{X})\mathcal{B}(\mathrm{W}^+ \to \mu^+\nu_\mu) &= 11.93 \pm 0.08\,(\mathrm{syst}) \pm 0.17\,(\mathrm{lumi})\,^{+0.07}_{-0.07}\,(\mathrm{acceptance})\,\mathrm{nb},\\
\sigma(\mathrm{pp} \to \mathrm{W}^-{+}\mathrm{X})\mathcal{B}(\mathrm{W}^- \to \mu^-\bar{\nu}_\mu) &= 8.86 \pm 0.06\,(\mathrm{syst}) \pm 0.12\,(\mathrm{lumi})\,^{+0.05}_{-0.06}\,(\mathrm{acceptance})\,\mathrm{nb},\\
\sigma(\mathrm{pp} \to \mathrm{Z} + \mathrm{X})\mathcal{B}(\mathrm{Z} \to \mu^+\mu^-) &= 2.021 \pm 0.009(\mathrm{syst}) \pm 0.028(\mathrm{lumi})\,^{+0.011}_{-0.013}\,(\mathrm{acceptance})\,\mathrm{nb},
\end{aligned}$$

with the uncertainty in the integrated luminosity (lumi), the uncertainty in the acceptance of the fiducial volume, and the remaining systematic uncertainty (syst), whereas the statistical component of the uncertainty is negligible. This translates into cross section ratios of:

$$\begin{aligned}
R^{\mathrm{W}^+/\mathrm{Z}} &= 5.906 \pm 0.004(\mathrm{stat}) \pm 0.040(\mathrm{syst})\,^{+0.022}_{-0.028}\,(\mathrm{acceptance}),\\
R^{\mathrm{W}^-/\mathrm{Z}} &= 4.382 \pm 0.003(\mathrm{stat}) \pm 0.029(\mathrm{syst})\,^{+0.023}_{-0.016}\,(\mathrm{acceptance}),\\
R^{\mathrm{W}^+/\mathrm{W}^-} &= 1.348 \pm 0.001(\mathrm{stat}) \pm 0.005(\mathrm{syst})\,^{+0.006}_{-0.007}\,(\mathrm{acceptance}),
\end{aligned}$$

where the statistical component of the uncertainty (stat) is not negligible anymore due to the decreased size of the systematic contributions to the uncertainty in the cross section ratios.

All results are in agreement with theoretical calculations at next-to-next-to-leading order accuracy in quantum chromodynamics plus next-to-next-to-leading logarithmic q_T resummation, where q_T is the transverse momentum of the W or Z boson. The high precision of the measurement highlights the excellent performance of the CMS detector following the long shutdown in 2018–2022, operating at the new center-of-mass energy of

JHEP01(2026)047

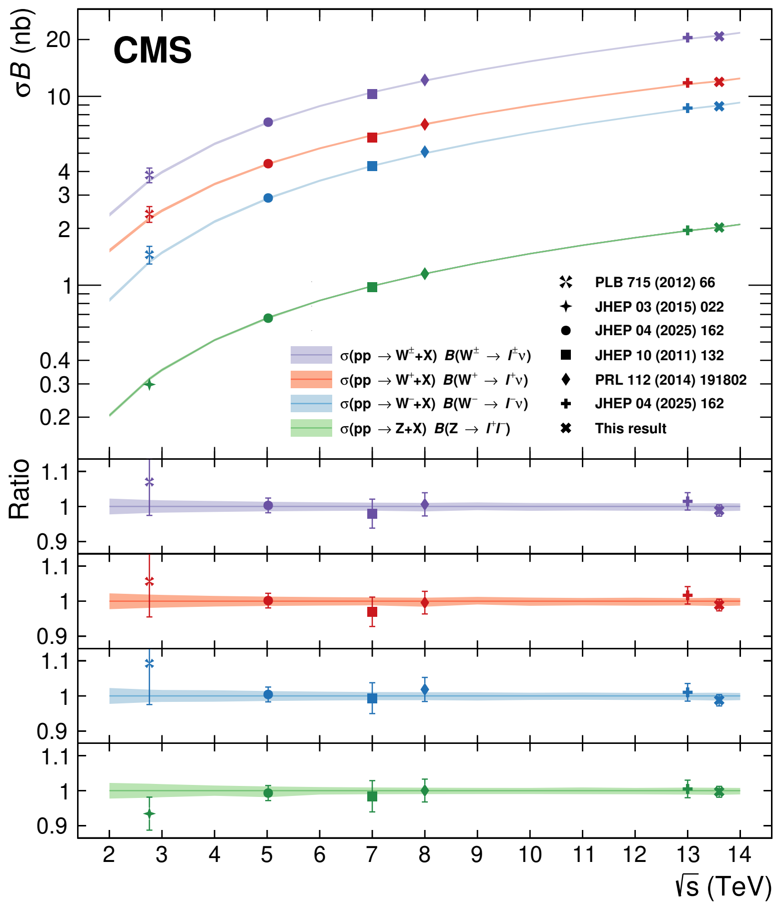

Figure 7. Comparison of measured products of total cross section and branching fractions for W and Z boson production at different center-of-mass energies with the corresponding theoretical prediction at NNLO+NNLL QCD accuracy obtained from DYTurbo. The uncertainties in the theoretical prediction include variations of the renormalization and factorization scales, as well as the PDF uncertainty evaluated with the NNPDF 3.1 set. The vertical uncertainty bars on the markers represent the total uncertainty of the measurement.

13.6 TeV. Moreover, the results underscore opportunities for refining the description of parton distribution functions and emphasize the potential value of dedicated differential measurements to enhance our understanding in the future.

Acknowledgments

We congratulate our colleagues in the CERN accelerator departments for the excellent performance of the LHC and thank the technical and administrative staffs at CERN and at other CMS institutes for their contributions to the success of the CMS effort. In addition, we gratefully acknowledge the computing centers and personnel of the Worldwide LHC Computing Grid and other centers for delivering so effectively the computing infrastructure essential to our analyses. Finally, we acknowledge the enduring support for the construction and operation of the LHC, the CMS detector, and the supporting computing infrastructure

JHEP01(2026)047

provided by the following funding agencies: SC (Armenia), BMBWF and FWF (Austria); FNRS and FWO (Belgium); CNPq, CAPES, FAPERJ, FAPERGS, and FAPESP (Brazil); MES and BNSF (Bulgaria); CERN; CAS, MoST, and NSFC (China); MINCIENCIAS (Colombia); MSES and CSF (Croatia); RIF (Cyprus); SENESCYT (Ecuador); ERC PRG, RVTT3 and MoER TK202 (Estonia); Academy of Finland, MEC, and HIP (Finland); CEA and CNRS/IN2P3 (France); SRNSF (Georgia); BMBF, DFG, and HGF (Germany); GSRI (Greece); NKFIH (Hungary); DAE and DST (India); IPM (Iran); SFI (Ireland); INFN (Italy); MSIP and NRF (Republic of Korea); MES (Latvia); LMTLT (Lithuania); MOE and UM (Malaysia); BUAP, CINVESTAV, CONACYT, LNS, SEP, and UASLP-FAI (Mexico); MOS (Montenegro); MBIE (New Zealand); PAEC (Pakistan); MES and NSC (Poland); FCT (Portugal); MESTD (Serbia); MICIU/AEI and PCTI (Spain); MOSTR (Sri Lanka); Swiss Funding Agencies (Switzerland); MST (Taipei); MHESI and NSTDA (Thailand); TUBITAK and TENMAK (Turkey); NASU (Ukraine); STFC (United Kingdom); DOE and NSF (USA).

Rachada-pisek Individuals have received support from the Marie-Curie program and the European Research Council and Horizon 2020 Grant, contract Nos. 675440, 724704, 752730, 758316, 765710, 824093, 101115353, 101002207, and COST Action CA16108 (European Union); the Leventis Foundation; the Alfred P. Sloan Foundation; the Alexander von Humboldt Foundation; the Science Committee, project no. 22rl-037 (Armenia); the Fonds pour la Formation à la Recherche dans l'Industrie et dans l'Agriculture (FRIA-Belgium); the Beijing Municipal Science & Technology Commission, No. Z191100007219010 and Fundamental Research Funds for the Central Universities (China); the Ministry of Education, Youth and Sports (MEYS) of the Czech Republic; the Shota Rustaveli National Science Foundation, grant FR-22-985 (Georgia); the Deutsche Forschungsgemeinschaft (DFG), among others, under Germany's Excellence Strategy — EXC 2121 "Quantum Universe" — 390833306, and under project number 400140256 — GRK2497; the Hellenic Foundation for Research and Innovation (HFRI), Project Number 2288 (Greece); the Hungarian Academy of Sciences, the New National Excellence Program — ÚNKP, the NKFIH research grants K 131991, K 133046, K 138136, K 143460, K 143477, K 146913, K 146914, K 147048, 2020-2.2.1-ED-2021-00181, TKP2021-NKTA-64, and 2021-4.1.2-NEMZ_KI-2024-00036 (Hungary); the Council of Science and Industrial Research, India; ICSC — National Research Center for High Performance Computing, Big Data and Quantum Computing and FAIR — Future Artificial Intelligence Research, funded by the NextGenerationEU program (Italy); the Latvian Council of Science; the Ministry of Education and Science, project no. 2022/WK/14, and the National Science Center, contracts Opus 2021/41/B/ST2/01369 and 2021/43/B/ST2/01552 (Poland); the Fundação para a Ciência e a Tecnologia, grant CEECIND/01334/2018 (Portugal); the National Priorities Research Program by Qatar National Research Fund; MICIU/AEI/10.13039/501100011033, ERDF/EU, "European Union NextGenerationEU/PRTR", and Programa Severo Ochoa del Principado de Asturias (Spain); the Chulalongkorn Academic into Its 2nd Century Project Advancement Project, and the National Science, Research and Innovation Fund via the Program Management Unit for Human Resources & Institutional Development, Research and Innovation, grant B39G670016 (Thailand); the Kavli Foundation; the Nvidia Corporation; the SuperMicro Corporation; the Welch Foundation, contract C-1845; and the Weston Havens Foundation (USA).

JHEP01(2026)047

Data Availability Statement. Release and preservation of data used by the CMS Collaboration as the basis for publications is guided by the CMS data preservation, re-use and open access policy, https://doi.org/10.7483/OPENDATA.CMS.1BNU.8V1W.

Code Availability Statement. The CMS core software is publicly available on GitHub https://github.com/cms-sw/cmssw.

References

[1] ATLAS collaboration, *Measurement of $W^{\pm}$-boson and Z-boson production cross-sections in pp collisions at $\sqrt{s} = 2.76$ TeV with the ATLAS detector*, Eur. Phys. J. C **79** (2019) 901 [arXiv:1907.03567] [INSPIRE].

[2] CMS collaboration, *Study of Z production in PbPb and pp collisions at $\sqrt{s_{\rm NN}} = 2.76$ TeV in the dimuon and dielectron decay channels*, JHEP **03** (2015) 022 [arXiv:1410.4825] [INSPIRE].

[3] ATLAS collaboration, *Measurements of W and Z boson production in pp collisions at $\sqrt{s} = 5.02$ TeV with the ATLAS detector*, Eur. Phys. J. C **79** (2019) 128 [Erratum ibid. **79** (2019) 374] [arXiv:1810.08424] [INSPIRE].

[4] CMS collaboration, *Measurement of the inclusive cross sections for W and Z boson production in proton-proton collisions at $\sqrt{s} = 5.02$ and 13 TeV*, JHEP **04** (2025) 162 [arXiv:2408.03744] [INSPIRE].

[5] ATLAS collaboration, *Precision measurement and interpretation of inclusive W^+, W^- and Z/γ^* production cross sections with the ATLAS detector*, Eur. Phys. J. C **77** (2017) 367 [arXiv:1612.03016] [INSPIRE].

[6] CMS collaboration, *Measurements of Inclusive W and Z Cross Sections in pp Collisions at $\sqrt{s} = 7$ TeV*, JHEP **01** (2011) 080 [arXiv:1012.2466] [INSPIRE].

[7] CMS collaboration, *Measurement of the Inclusive W and Z Production Cross Sections in pp Collisions at $\sqrt{s} = 7$ TeV*, JHEP **10** (2011) 132 [arXiv:1107.4789] [INSPIRE].

[8] LHCb collaboration, *Measurement of the forward W boson cross-section in pp collisions at $\sqrt{s} = 7$ TeV*, JHEP **12** (2014) 079 [arXiv:1408.4354] [INSPIRE].

[9] LHCb collaboration, *Measurement of the cross-section for $Z \to e^+e^-$ production in pp collisions at $\sqrt{s} = 7$ TeV*, JHEP **02** (2013) 106 [arXiv:1212.4620] [INSPIRE].

[10] LHCb collaboration, *Measurement of the forward Z boson production cross-section in pp collisions at $\sqrt{s} = 7$ TeV*, JHEP **08** (2015) 039 [arXiv:1505.07024] [INSPIRE].

[11] LHCb collaboration, *Measurement of forward $W \to e\nu$ production in pp collisions at $\sqrt{s} = 8$ TeV*, JHEP **10** (2016) 030 [arXiv:1608.01484] [INSPIRE].

[12] LHCb collaboration, *Measurement of the forward Z boson production cross-section in pp collisions at $\sqrt{s} = 13$ TeV*, JHEP **09** (2016) 136 [arXiv:1607.06495] [INSPIRE].

[13] LHCb collaboration, *Measurement of forward W and Z boson production in pp collisions at $\sqrt{s} = 8$ TeV*, JHEP **01** (2016) 155 [arXiv:1511.08039] [INSPIRE].

[14] CMS collaboration, *Measurement of Inclusive W and Z Boson Production Cross Sections in pp Collisions at $\sqrt{s} = 8$ TeV*, *Phys. Rev. Lett.* **112** (2014) 191802 [arXiv:1402.0923] [INSPIRE].

[15] ATLAS collaboration, *Measurement of $W^{\pm}$ and Z-boson production cross sections in pp collisions at $\sqrt{s} = 13$ TeV with the ATLAS detector*, *Phys. Lett. B* **759** (2016) 601 [arXiv:1603.09222] [INSPIRE].

[16] ATLAS collaboration, *Measurement of vector boson production cross sections and their ratios using pp collisions at $\sqrt{s} = 13.6$ TeV with the ATLAS detector*, *Phys. Lett. B* **854** (2024) 138725 [arXiv:2403.12902] [INSPIRE].

[17] HEPData record for this analysis, https://doi.org/10.17182/hepdata.157226 (2025).

[18] CMS collaboration, *The CMS Experiment at the CERN LHC*, 2008 *JINST* **3** S08004 [INSPIRE].

[19] CMS collaboration, *Development of the CMS detector for the CERN LHC Run 3*, 2024 *JINST* **19** P05064 [arXiv:2309.05466] [INSPIRE].

[20] CMS collaboration, *Performance of the CMS Level-1 trigger in proton-proton collisions at $\sqrt{s} = 13$ TeV*, 2020 *JINST* **15** P10017 [arXiv:2006.10165] [INSPIRE].

[21] CMS collaboration, *The CMS trigger system*, 2017 *JINST* **12** P01020 [arXiv:1609.02366] [INSPIRE].

[22] CMS collaboration, *Performance of the CMS high-level trigger during LHC Run 2*, 2024 *JINST* **19** P11021 [arXiv:2410.17038] [INSPIRE].

[23] CMS collaboration, *Particle-flow reconstruction and global event description with the CMS detector*, 2017 *JINST* **12** P10003 [arXiv:1706.04965] [INSPIRE].

[24] D. Contardo et al., *Technical Proposal for the Phase-II Upgrade of the CMS Detector*, hrefhttps://cds.cern.ch/record/2020886CERN-LHCC-2015-010 (2015) [INSPIRE].

[25] CMS collaboration, *Performance of missing transverse momentum reconstruction in proton-proton collisions at $\sqrt{s} = 13$ TeV using the CMS detector*, 2019 *JINST* **14** P07004 [arXiv:1903.06078] [INSPIRE].

[26] J. Alwall et al., *The automated computation of tree-level and next-to-leading order differential cross sections, and their matching to parton shower simulations*, *JHEP* **07** (2014) 079 [arXiv:1405.0301] [INSPIRE].

[27] R. Frederix and S. Frixione, *Merging meets matching in MC@NLO*, *JHEP* **12** (2012) 061 [arXiv:1209.6215] [INSPIRE].

[28] P. Nason, *A New method for combining NLO QCD with shower Monte Carlo algorithms*, *JHEP* **11** (2004) 040 [hep-ph/0409146] [INSPIRE].

[29] S. Frixione, P. Nason and C. Oleari, *Matching NLO QCD computations with Parton Shower simulations: the POWHEG method*, *JHEP* **11** (2007) 070 [arXiv:0709.2092] [INSPIRE].

[30] S. Alioli, P. Nason, C. Oleari and E. Re, *A general framework for implementing NLO calculations in shower Monte Carlo programs: the POWHEG BOX*, *JHEP* **06** (2010) 043 [arXiv:1002.2581] [INSPIRE].

[31] R. Frederix, E. Re and P. Torrielli, *Single-top t-channel hadroproduction in the four-flavour scheme with POWHEG and aMC@NLO*, *JHEP* **09** (2012) 130 [arXiv:1207.5391] [INSPIRE].

[32] E. Re, *Single-top Wt-channel production matched with parton showers using the POWHEG method*, *Eur. Phys. J. C* **71** (2011) 1547 [arXiv:1009.2450] [INSPIRE].

[33] P. Nason and G. Zanderighi, *W^+W^-, WZ and ZZ production in the POWHEG-BOX-V2*, Eur. Phys. J. C **74** (2014) 2702 [arXiv:1311.1365] [INSPIRE].

[34] P. Artoisenet, R. Frederix, O. Mattelaer and R. Rietkerk, *Automatic spin-entangled decays of heavy resonances in Monte Carlo simulations*, JHEP **03** (2013) 015 [arXiv:1212.3460] [INSPIRE].

[35] C. Bierlich et al., *A comprehensive guide to the physics and usage of PYTHIA 8.3*, SciPost Phys. Codeb. **2022** (2022) 8 [arXiv:2203.11601] [INSPIRE].

[36] CMS collaboration, *Extraction and validation of a new set of CMS PYTHIA8 tunes from underlying-event measurements*, Eur. Phys. J. C **80** (2020) 4 [arXiv:1903.12179] [INSPIRE].

[37] NNPDF collaboration, *Parton distributions from high-precision collider data*, Eur. Phys. J. C **77** (2017) 663 [arXiv:1706.00428] [INSPIRE].

[38] GEANT4 collaboration, *GEANT4 — A Simulation Toolkit*, Nucl. Instrum. Meth. A **506** (2003) 250 [INSPIRE].

[39] CMS collaboration, *Performance of the CMS muon detector and muon reconstruction with proton-proton collisions at $\sqrt{s} = 13$ TeV*, 2018 JINST **13** P06015 [arXiv:1804.04528] [INSPIRE].

[40] CMS collaboration, *Electron and photon reconstruction and identification with the CMS experiment at the CERN LHC*, 2021 JINST **16** P05014 [arXiv:2012.06888] [INSPIRE].

[41] CMS collaboration, *ECAL 2016 refined calibration and Run2 summary plots*, https://cds.cern.ch/record/2717925CMS-DP-2020-021 (2020).

[42] CMS collaboration, *High-precision measurement of the W boson mass with the CMS experiment at the LHC*, arXiv:2412.13872 [INSPIRE].

[43] S. Camarda et al., *DYTurbo: Fast predictions for Drell-Yan processes*, Eur. Phys. J. C **80** (2020) 251 [*Erratum ibid.* **80** (2020) 440] [arXiv:1910.07049] [INSPIRE].

[44] S. Camarda, L. Cieri and G. Ferrera, *Drell-Yan lepton-pair production: qT resummation at N3LL accuracy and fiducial cross sections at N3LO*, Phys. Rev. D **104** (2021) L111503 [arXiv:2103.04974] [INSPIRE].

[45] S. Camarda, L. Cieri and G. Ferrera, *Fiducial perturbative power corrections within the q_T subtraction formalism*, Eur. Phys. J. C **82** (2022) 575 [arXiv:2111.14509] [INSPIRE].

[46] S. Camarda, L. Cieri and G. Ferrera, *Drell-Yan lepton-pair production: qT resummation at N4LL accuracy*, Phys. Lett. B **845** (2023) 138125 [arXiv:2303.12781] [INSPIRE].

[47] CMS collaboration, *Performance of the CMS muon trigger system in proton-proton collisions at $\sqrt{s} = 13$ TeV*, 2021 JINST **16** P07001 [arXiv:2102.04790] [INSPIRE].

[48] M. Oreglia, *A Study of the Reactions $\psi' \to \gamma\gamma\psi$*, PhD. thesis, Stanford University, Stanford, U.S.A. (1980), https://www.slac.stanford.edu/cgi-bin/getdoc/slac-r-236.pdf [INSPIRE].

[49] J.E. Gaiser, *Charmonium Spectroscopy From Radiative Decays of the J/ψ and ψ'*, PhD. thesis, Stanford University, Stanford, U.S.A. (1982), https://www.slac.stanford.edu/cgi-bin/getdoc/slac-r-255.pdf [INSPIRE].

[50] CMS collaboration, *The CMS Statistical Analysis and Combination Tool: Combine*, Comput. Softw. Big Sci. **8** (2024) 19 [arXiv:2404.06614] [INSPIRE].

[51] W. Verkerke and D.P. Kirkby, *The RooFit toolkit for data modeling*, *eConf C* **0303241** (2003) MOLT007 [physics/0306116] [INSPIRE].

[52] L. Moneta et al., *The RooStats Project*, *PoS* **ACAT2010** (2010) 057 [arXiv:1009.1003] [INSPIRE].

[53] CMS collaboration, *First measurement of the top quark pair production cross section in proton-proton collisions at* $\sqrt{s} = 13.6$ *TeV*, *JHEP* **08** (2023) 204 [arXiv:2303.10680] [INSPIRE].

[54] J. Campbell, T. Neumann and Z. Sullivan, *Single-top-quark production in the t-channel at NNLO*, *JHEP* **02** (2021) 040 [arXiv:2012.01574] [INSPIRE].

[55] J.S. Conway, *Incorporating Nuisance Parameters in Likelihoods for Multisource Spectra*, in the proceedings of the *PHYSTAT 2011*, Geneva, Switzerland (2011) [DOI:10.5170/CERN-2011-006.115] [arXiv:1103.0354] [INSPIRE].

[56] R.J. Barlow and C. Beeston, *Fitting using finite Monte Carlo samples*, *Comput. Phys. Commun.* **77** (1993) 219 [INSPIRE].

[57] CMS collaboration, *Precision luminosity measurement in proton-proton collisions at* $\sqrt{s} = 13$ *TeV in 2015 and 2016 at CMS*, *Eur. Phys. J. C* **81** (2021) 800 [arXiv:2104.01927] [INSPIRE].

[58] CMS collaboration, *Luminosity measurement in proton-proton collisions at* 13.6 TeV *in 2022 at CMS*, CMS-PAS-LUM-22-001 (2024) [INSPIRE].

[59] T.-J. Hou et al., *New CTEQ global analysis of quantum chromodynamics with high-precision data from the LHC*, *Phys. Rev. D* **103** (2021) 014013 [arXiv:1912.10053] [INSPIRE].

[60] S. Bailey et al., *Parton distributions from LHC, HERA, Tevatron and fixed target data: MSHT20 PDFs*, *Eur. Phys. J. C* **81** (2021) 341 [arXiv:2012.04684] [INSPIRE].

JHEP01(2026)047

The CMS collaboration

Yerevan Physics Institute, Yerevan, Armenia
V. Chekhovsky, A. Hayrapetyan, V. Makarenko, A. Tumasyan[1]

Institut für Hochenergiephysik, Vienna, Austria
W. Adam, J.W. Andrejkovic, L. Benato, T. Bergauer, S. Chatterjee, K. Damanakis, M. Dragicevic, P.S. Hussain, M. Jeitler[2], N. Krammer, A. Li, D. Liko, I. Mikulec, J. Schieck[2], R. Schöfbeck[2], D. Schwarz, M. Sonawane, W. Waltenberger, C.-E. Wulz[2]

Universiteit Antwerpen, Antwerpen, Belgium
T. Janssen, H. Kwon, T. Van Laer, P. Van Mechelen

Vrije Universiteit Brussel, Brussel, Belgium
N. Breugelmans, J. D'Hondt, S. Dansana, A. De Moor, M. Delcourt, F. Heyen, Y. Hong, S. Lowette, I. Makarenko, D. Müller, S. Tavernier, M. Tytgat[3], G.P. Van Onsem, S. Van Putte, D. Vannerom

Université Libre de Bruxelles, Bruxelles, Belgium
B. Bilin, B. Clerbaux, A.K. Das, I. De Bruyn, G. De Lentdecker, H. Evard, L. Favart, P. Gianneios, A. Khalilzadeh, F.A. Khan, A. Malara, M.A. Shahzad, L. Thomas, M. Vanden Bemden, C. Vander Velde, P. Vanlaer

Ghent University, Ghent, Belgium
M. De Coen, D. Dobur, G. Gokbulut, J. Knolle, L. Lambrecht, D. Marckx, K. Skovpen, N. Van Den Bossche, J. van der Linden, J. Vandenbroeck, L. Wezenbeek

Université Catholique de Louvain, Louvain-la-Neuve, Belgium
S. Bein, A. Benecke, A. Bethani, G. Bruno, C. Caputo, J. De Favereau De Jeneret, C. Delaere, I.S. Donertas, A. Giammanco, A.O. Guzel, Sa. Jain, V. Lemaitre, J. Lidrych, P. Mastrapasqua, T.T. Tran, S. Turkcapar

Centro Brasileiro de Pesquisas Fisicas, Rio de Janeiro, Brazil
G.A. Alves, E. Coelho, G. Correia Silva, C. Hensel, T. Menezes De Oliveira, C. Mora Herrera[4], P. Rebello Teles, M. Soeiro, E.J. Tonelli Manganote[5], A. Vilela Pereira[4]

Universidade do Estado do Rio de Janeiro, Rio de Janeiro, Brazil
W.L. Aldá Júnior, M. Barroso Ferreira Filho, H. Brandao Malbouisson, W. Carvalho, J. Chinellato[6], E.M. Da Costa, G.G. Da Silveira[7], D. De Jesus Damiao, S. Fonseca De Souza, R. Gomes De Souza, T. Laux Kuhn[7], M. Macedo, J. Martins, K. Mota Amarilo, L. Mundim, H. Nogima, J.P. Pinheiro, A. Santoro, A. Sznajder, M. Thiel

Universidade Estadual Paulista, Universidade Federal do ABC, São Paulo, Brazil
C.A. Bernardes[7], L. Calligaris, T.R. Fernandez Perez Tomei, E.M. Gregores, I. Maietto Silverio, P.G. Mercadante, S.F. Novaes, B. Orzari, Sandra S. Padula, V. Scheurer

JHEP01(2026)047

Institute for Nuclear Research and Nuclear Energy, Bulgarian Academy of Sciences, Sofia, Bulgaria
A. Aleksandrov, G. Antchev, R. Hadjiiska, P. Iaydjiev, M. Misheva, M. Shopova, G. Sultanov

University of Sofia, Sofia, Bulgaria
A. Dimitrov, L. Litov, B. Pavlov, P. Petkov, A. Petrov, E. Shumka

Instituto De Alta Investigación, Universidad de Tarapacá, Casilla 7 D, Arica, Chile
S. Keshri, D. Laroze, S. Thakur

Beihang University, Beijing, China
T. Cheng, T. Javaid, L. Yuan

Department of Physics, Tsinghua University, Beijing, China
Z. Hu, Z. Liang, J. Liu

Institute of High Energy Physics, Beijing, China
G.M. Chen[8], H.S. Chen[8], M. Chen[8], F. Iemmi, C.H. Jiang, A. Kapoor[9], H. Liao, Z.-A. Liu[10], R. Sharma[11], J.N. Song[10], J. Tao, C. Wang[8], J. Wang, Z. Wang[8], H. Zhang, J. Zhao

State Key Laboratory of Nuclear Physics and Technology, Peking University, Beijing, China
A. Agapitos, Y. Ban, A. Carvalho Antunes De Oliveira, S. Deng, B. Guo, C. Jiang, A. Levin, C. Li, Q. Li, Y. Mao, S. Qian, S.J. Qian, X. Qin, X. Sun, D. Wang, H. Yang, Y. Zhao, C. Zhou

Guangdong Provincial Key Laboratory of Nuclear Science and Guangdong-Hong Kong Joint Laboratory of Quantum Matter, South China Normal University, Guangzhou, China
S. Yang

Sun Yat-Sen University, Guangzhou, China
Z. You

University of Science and Technology of China, Hefei, China
K. Jaffel, N. Lu

Nanjing Normal University, Nanjing, China
G. Bauer[12], B. Li[13], H. Wang, K. Yi[14], J. Zhang

Institute of Modern Physics and Key Laboratory of Nuclear Physics and Ion-beam Application (MOE) - Fudan University, Shanghai, China
Y. Li

JHEP01(2026)047

Zhejiang University, Hangzhou, Zhejiang, China
Z. Lin, C. Lu, M. Xiao

Universidad de Los Andes, Bogota, Colombia
C. Avila, D.A. Barbosa Trujillo, A. Cabrera, C. Florez, J. Fraga, J.A. Reyes Vega

Universidad de Antioquia, Medellin, Colombia
J. Jaramillo, C. Rendón, M. Rodriguez, A.A. Ruales Barbosa, J.D. Ruiz Alvarez

University of Split, Faculty of Electrical Engineering, Mechanical Engineering and Naval Architecture, Split, Croatia
D. Giljanovic, N. Godinovic, D. Lelas, A. Sculac

University of Split, Faculty of Science, Split, Croatia
M. Kovac, A. Petkovic, T. Sculac

Institute Rudjer Boskovic, Zagreb, Croatia
P. Bargassa, V. Brigljevic, B.K. Chitroda, D. Ferencek, K. Jakovcic, A. Starodumov[15], T. Susa

University of Cyprus, Nicosia, Cyprus
A. Attikis, K. Christoforou, A. Hadjiagapiou, C. Leonidou, J. Mousa, C. Nicolaou, L. Paizanos, F. Ptochos, P.A. Razis, H. Rykaczewski, H. Saka, A. Stepennov

Charles University, Prague, Czech Republic
M. Finger, M. Finger Jr., A. Kveton

Escuela Politecnica Nacional, Quito, Ecuador
E. Ayala

Universidad San Francisco de Quito, Quito, Ecuador
E. Carrera Jarrin

Academy of Scientific Research and Technology of the Arab Republic of Egypt, Egyptian Network of High Energy Physics, Cairo, Egypt
A.A. Abdelalim[16,17], S. Elgammal[18], A. Ellithi Kamel[19]

Center for High Energy Physics (CHEP-FU), Fayoum University, El-Fayoum, Egypt
M. Abdullah Al-Mashad, M.A. Mahmoud

National Institute of Chemical Physics and Biophysics, Tallinn, Estonia
K. Ehataht, M. Kadastik, T. Lange, C. Nielsen, J. Pata, M. Raidal, L. Tani, C. Veelken

Department of Physics, University of Helsinki, Helsinki, Finland
K. Osterberg, M. Voutilainen

JHEP01(2026)047

Helsinki Institute of Physics, Helsinki, Finland

N. Bin Norjoharuddeen, E. Brücken, F. Garcia, P. Inkaew, K.T.S. Kallonen, T. Lampén, K. Lassila-Perini, S. Lehti, T. Lindén, M. Myllymäki, M.m. Rantanen, J. Tuominiemi

Lappeenranta-Lahti University of Technology, Lappeenranta, Finland

H. Kirschenmann, P. Luukka, H. Petrow

IRFU, CEA, Université Paris-Saclay, Gif-sur-Yvette, France

M. Besancon, F. Couderc, M. Dejardin, D. Denegri, J.L. Faure, F. Ferri, S. Ganjour, P. Gras, G. Hamel de Monchenault, M. Kumar, V. Lohezic, J. Malcles, F. Orlandi, L. Portales, A. Rosowsky, M.Ö. Sahin, A. Savoy-Navarro[20], P. Simkina, M. Titov, M. Tornago

Laboratoire Leprince-Ringuet, CNRS/IN2P3, Ecole Polytechnique, Institut Polytechnique de Paris, Palaiseau, France

F. Beaudette, G. Boldrini, P. Busson, A. Cappati, C. Charlot, M. Chiusi, T.D. Cuisset, F. Damas, O. Davignon, A. De Wit, I.T. Ehle, B.A. Fontana Santos Alves, S. Ghosh, A. Gilbert, R. Granier de Cassagnac, B. Harikrishnan, L. Kalipoliti, G. Liu, M. Manoni, M. Nguyen, S. Obraztsov, C. Ochando, R. Salerno, J.B. Sauvan, Y. Sirois, G. Sokmen, L. Urda Gómez, E. Vernazza, A. Zabi, A. Zghiche

Université de Strasbourg, CNRS, IPHC UMR 7178, Strasbourg, France

J.-L. Agram[21], J. Andrea, D. Bloch, J.-M. Brom, E.C. Chabert, C. Collard, S. Falke, U. Goerlach, R. Haeberle, A.-C. Le Bihan, M. Meena, O. Poncet, G. Saha, M.A. Sessini, P. Van Hove, P. Vaucelle

Centre de Calcul de l'Institut National de Physique Nucleaire et de Physique des Particules, CNRS/IN2P3, Villeurbanne, France

A. Di Florio

Institut de Physique des 2 Infinis de Lyon (IP2I), Villeurbanne, France

D. Amram, S. Beauceron, B. Blancon, G. Boudoul, N. Chanon, D. Contardo, P. Depasse, C. Dozen[22], H. El Mamouni, J. Fay, S. Gascon, M. Gouzevitch, C. Greenberg, G. Grenier, B. Ille, E. Jourd'huy, I.B. Laktineh, M. Lethuillier, L. Mirabito, S. Perries, A. Purohit, M. Vander Donckt, P. Verdier, J. Xiao

Georgian Technical University, Tbilisi, Georgia

I. Lomidze, T. Toriashvili[23], Z. Tsamalaidze[24]

RWTH Aachen University, I. Physikalisches Institut, Aachen, Germany

V. Botta, S. Consuegra Rodríguez, L. Feld, K. Klein, M. Lipinski, D. Meuser, A. Pauls, D. Pérez Adán, N. Röwert, M. Teroerde

RWTH Aachen University, III. Physikalisches Institut A, Aachen, Germany

S. Diekmann, A. Dodonova, N. Eich, D. Eliseev, F. Engelke, J. Erdmann, M. Erdmann, B. Fischer, T. Hebbeker, K. Hoepfner, F. Ivone, A. Jung, M.y. Lee,

F. Mausolf, M. Merschmeyer, A. Meyer, S. Mukherjee, F. Nowotny, A. Pozdnyakov, Y. Rath, W. Redjeb, F. Rehm, H. Reithler, V. Sarkisovi, A. Schmidt, C. Seth, A. Sharma, J.L. Spah, F. Torres Da Silva De Araujo[25], S. Wiedenbeck, S. Zaleski

RWTH Aachen University, III. Physikalisches Institut B, Aachen, Germany
C. Dziwok, G. Flügge, T. Kress, A. Nowack, O. Pooth, A. Stahl, T. Ziemons, A. Zotz

Deutsches Elektronen-Synchrotron, Hamburg, Germany
H. Aarup Petersen, M. Aldaya Martin, J. Alimena, S. Amoroso, Y. An, J. Bach, S. Baxter, M. Bayatmakou, H. Becerril Gonzalez, O. Behnke, A. Belvedere, F. Blekman[26], K. Borras[27], A. Campbell, A. Cardini, F. Colombina, M. De Silva, G. Eckerlin, D. Eckstein, L.I. Estevez Banos, E. Gallo[26], A. Geiser, V. Guglielmi, M. Guthoff, A. Hinzmann, L. Jeppe, B. Kaech, M. Kasemann, C. Kleinwort, R. Kogler, M. Komm, D. Krücker, W. Lange, D. Leyva Pernia, K. Lipka[28], W. Lohmann[29], F. Lorkowski, R. Mankel, I.-A. Melzer-Pellmann, M. Mendizabal Morentin, A.B. Meyer, G. Milella, K. Moral Figueroa, A. Mussgiller, L.P. Nair, J. Niedziela, A. Nürnberg, J. Park, E. Ranken, A. Raspereza, D. Rastorguev, J. Rübenach, L. Rygaard, M. Scham[30,27], S. Schnake[27], P. Schütze, C. Schwanenberger[26], D. Selivanova, K. Sharko, M. Shchedrolosiev, D. Stafford, F. Vazzoler, A. Ventura Barroso, R. Walsh, D. Wang, Q. Wang, K. Wichmann, L. Wiens[27], C. Wissing, Y. Yang, S. Zakharov, A. Zimermmane Castro Santos

University of Hamburg, Hamburg, Germany
A. Albrecht, S. Albrecht, M. Antonello, S. Bollweg, M. Bonanomi, P. Connor, K. El Morabit, Y. Fischer, E. Garutti, A. Grohsjean, J. Haller, D. Hundhausen, H.R. Jabusch, G. Kasieczka, P. Keicher, R. Klanner, W. Korcari, T. Kramer, C.c. Kuo, V. Kutzner, F. Labe, J. Lange, A. Lobanov, C. Matthies, L. Moureaux, M. Mrowietz, A. Nigamova, Y. Nissan, A. Paasch, K.J. Pena Rodriguez, T. Quadfasel, B. Raciti, M. Rieger, D. Savoiu, J. Schindler, P. Schleper, M. Schröder, J. Schwandt, M. Sommerhalder, H. Stadie, G. Steinbrück, A. Tews, B. Wiederspan, M. Wolf

Karlsruher Institut fuer Technologie, Karlsruhe, Germany
S. Brommer, E. Butz, T. Chwalek, A. Dierlamm, G.G. Dincer, U. Elicabuk, N. Faltermann, M. Giffels, A. Gottmann, F. Hartmann[31], R. Hofsaess, M. Horzela, U. Husemann, J. Kieseler, M. Klute, O. Lavoryk, J.M. Lawhorn, M. Link, A. Lintuluoto, S. Maier, M. Mormile, Th. Müller, M. Neukum, M. Oh, E. Pfeffer, M. Presilla, G. Quast, K. Rabbertz, B. Regnery, R. Schmieder, N. Shadskiy, I. Shvetsov, H.J. Simonis, L. Sowa, L. Stockmeier, K. Tauqeer, M. Toms, B. Topko, N. Trevisani, T. Voigtländer, R.F. Von Cube, J. Von Den Driesch, M. Wassmer, S. Wieland, F. Wittig, R. Wolf, X. Zuo

Institute of Nuclear and Particle Physics (INPP), NCSR Demokritos, Aghia Paraskevi, Greece
G. Anagnostou, G. Daskalakis, A. Kyriakis, A. Papadopoulos[31], A. Stakia

JHEP01(2026)047

National and Kapodistrian University of Athens, Athens, Greece
G. Melachroinos, Z. Painesis, I. Paraskevas, N. Saoulidou, K. Theofilatos, E. Tziaferi, K. Vellidis, I. Zisopoulos

National Technical University of Athens, Athens, Greece
G. Bakas, T. Chatzistavrou, G. Karapostoli, K. Kousouris, I. Papakrivopoulos, E. Siamarkou, G. Tsipolitis

University of Ioánnina, Ioánnina, Greece
I. Bestintzanos, I. Evangelou, C. Foudas, C. Kamtsikis, P. Katsoulis, P. Kokkas, P.G. Kosmoglou Kioseoglou, N. Manthos, I. Papadopoulos, J. Strologas

HUN-REN Wigner Research Centre for Physics, Budapest, Hungary
C. Hajdu, D. Horvath[32,33], K. Márton, A.J. Rádl[34], F. Sikler, V. Veszpremi

MTA-ELTE Lendület CMS Particle and Nuclear Physics Group, Eötvös Loránd University, Budapest, Hungary
M. Csanád, K. Farkas, A. Fehérkuti[35], M.M.A. Gadallah[36], Á. Kadlecsik, P. Major, G. Pásztor, G.I. Veres

Faculty of Informatics, University of Debrecen, Debrecen, Hungary
B. Ujvari, G. Zilizi

HUN-REN ATOMKI - Institute of Nuclear Research, Debrecen, Hungary
G. Bencze, S. Czellar, J. Molnar, Z. Szillasi

Karoly Robert Campus, MATE Institute of Technology, Gyongyos, Hungary
T. Csorgo[35], F. Nemes[35], T. Novak

Panjab University, Chandigarh, India
S. Bansal, S.B. Beri, V. Bhatnagar, G. Chaudhary, S. Chauhan, N. Dhingra[37], A. Kaur, A. Kaur, H. Kaur, M. Kaur, S. Kumar, T. Sheokand, J.B. Singh, A. Singla

University of Delhi, Delhi, India
A. Bhardwaj, A. Chhetri, B.C. Choudhary, A. Kumar, A. Kumar, M. Naimuddin, K. Ranjan, M.K. Saini, S. Saumya

Saha Institute of Nuclear Physics, HBNI, Kolkata, India
S. Baradia, S. Barman[38], S. Bhattacharya, S. Das Gupta, S. Dutta, S. Dutta, S. Sarkar

Indian Institute of Technology Madras, Madras, India
M.M. Ameen, P.K. Behera, S.C. Behera, S. Chatterjee, G. Dash, P. Jana, P. Kalbhor, S. Kamble, J.R. Komaragiri[39], D. Kumar[39], T. Mishra, B. Parida[40], P.R. Pujahari, N.R. Saha, A.K. Sikdar, R.K. Singh, P. Verma, S. Verma, A. Vijay

Tata Institute of Fundamental Research-A, Mumbai, India
S. Dugad, G.B. Mohanty, M. Shelake, P. Suryadevara

JHEP01(2026)047

Tata Institute of Fundamental Research-B, Mumbai, India
A. Bala, S. Banerjee, S. Bhowmik, R.M. Chatterjee, M. Guchait, Sh. Jain, A. Jaiswal, B.M. Joshi, S. Kumar, G. Majumder, K. Mazumdar, S. Parolia, A. Thachayath

National Institute of Science Education and Research, An OCC of Homi Bhabha National Institute, Bhubaneswar, Odisha, India
S. Bahinipati[41], C. Kar, D. Maity[42], P. Mal, K. Naskar[42], A. Nayak[42], S. Nayak, K. Pal, P. Sadangi, S.K. Swain, S. Varghese[42], D. Vats[42]

Indian Institute of Science Education and Research (IISER), Pune, India
S. Acharya[43], A. Alpana, S. Dube, B. Gomber[43], P. Hazarika, B. Kansal, A. Laha, B. Sahu[43], S. Sharma, K.Y. Vaish

Isfahan University of Technology, Isfahan, Iran
H. Bakhshiansohi[44], A. Jafari[45], M. Zeinali[46]

Institute for Research in Fundamental Sciences (IPM), Tehran, Iran
S. Bashiri, S. Chenarani[47], S.M. Etesami, Y. Hosseini, M. Khakzad, E. Khazaie, M. Mohammadi Najafabadi, S. Tizchang[48]

University College Dublin, Dublin, Ireland
M. Felcini, M. Grunewald

INFN Sezione di Bari[a], Università di Bari[b], Politecnico di Bari[c], Bari, Italy
M. Abbrescia[a,b], A. Colaleo[a,b], D. Creanza[a,c], B. D'Anzi[a,b], N. De Filippis[a,c], M. De Palma[a,b], W. Elmetenawee[a,b,16], N. Ferrara[a,b], L. Fiore[a], G. Iaselli[a,c], L. Longo[a], M. Louka[a,b], G. Maggi[a,c], M. Maggi[a], I. Margjeka[a], V. Mastrapasqua[a,b], S. My[a,b], S. Nuzzo[a,b], A. Pellecchia[a,b], A. Pompili[a,b], G. Pugliese[a,c], R. Radogna[a,b], D. Ramos[a], A. Ranieri[a], L. Silvestris[a], F.M. Simone[a,c], Ü. Sözbilir[a], A. Stamerra[a,b], D. Troiano[a,b], R. Venditti[a,b], P. Verwilligen[a], A. Zaza[a,b]

INFN Sezione di Bologna[a], Università di Bologna[b], Bologna, Italy
G. Abbiendi[a], C. Battilana[a,b], D. Bonacorsi[a,b], P. Capiluppi[a,b], A. Castro[†,a,b], F.R. Cavallo[a], M. Cuffiani[a,b], G.M. Dallavalle[a], T. Diotalevi[a,b], F. Fabbri[a], A. Fanfani[a,b], D. Fasanella[a], P. Giacomelli[a], L. Giommi[a,b], C. Grandi[a], L. Guiducci[a,b], S. Lo Meo[a,49], M. Lorusso[a,b], L. Lunerti[a], S. Marcellini[a], G. Masetti[a], F.L. Navarria[a,b], G. Paggi[a,b], A. Perrotta[a], F. Primavera[a,b], A.M. Rossi[a,b], S. Rossi Tisbeni[a,b], T. Rovelli[a,b], G.P. Siroli[a,b]

INFN Sezione di Catania[a], Università di Catania[b], Catania, Italy
S. Costa[a,b,50], A. Di Mattia[a], A. Lapertosa[a], R. Potenza[a,b], A. Tricomi[a,b,50]

INFN Sezione di Firenze[a], Università di Firenze[b], Firenze, Italy
P. Assiouras[a], G. Barbagli[a], G. Bardelli[a,b], B. Camaiani[a,b], A. Cassese[a], R. Ceccarelli[a], V. Ciulli[a,b], C. Civinini[a], R. D'Alessandro[a,b], E. Focardi[a,b], T. Kello[a], G. Latino[a,b],

JHEP01(2026)047

P. Lenzi[a,b], M. Lizzo[a], M. Meschini[a], S. Paoletti[a], A. Papanastassiou[a,b], G. Sguazzoni[a], L. Viliani[a]

INFN Laboratori Nazionali di Frascati, Frascati, Italy
L. Benussi, S. Bianco, S. Meola[51], D. Piccolo

INFN Sezione di Genova[a], Università di Genova[b], Genova, Italy
M. Alves Gallo Pereira[a], F. Ferro[a], E. Robutti[a], S. Tosi[a,b]

INFN Sezione di Milano-Bicocca[a], Università di Milano-Bicocca[b], Milano, Italy
A. Benaglia[a], F. Brivio[a], F. Cetorelli[a,b], F. De Guio[a,b], M.E. Dinardo[a,b], P. Dini[a], S. Gennai[a], R. Gerosa[a,b], A. Ghezzi[a,b], P. Govoni[a,b], L. Guzzi[a], G. Lavizzari[a,b], M.T. Lucchini[a,b], M. Malberti[a], S. Malvezzi[a], A. Massironi[a], D. Menasce[a], L. Moroni[a], M. Paganoni[a,b], S. Palluotto[a,b], D. Pedrini[a], A. Perego[a,b], B.S. Pinolini[a], G. Pizzati[a,b], S. Ragazzi[a,b], T. Tabarelli de Fatis[a,b]

INFN Sezione di Napoli[a], Università di Napoli 'Federico II'[b], Napoli, Italy; Università della Basilicata[c], Potenza, Italy; Scuola Superiore Meridionale (SSM)[d], Napoli, Italy
S. Buontempo[a], A. Cagnotta[a,b], F. Carnevali[a,b], N. Cavallo[a,c], F. Fabozzi[a,c], A.O.M. Iorio[a,b], L. Lista[a,b,52], P. Paolucci[a,31], B. Rossi[a]

INFN Sezione di Padova[a], Università di Padova[b], Padova, Italy; Università di Trento[c], Trento, Italy
R. Ardino[a], P. Azzi[a], N. Bacchetta[a,53], M. Bellato[a], P. Bortignon[a], G. Bortolato[a,b], A.C.M. Bulla[a], R. Carlin[a,b], P. Checchia[a], T. Dorigo[a,54], F. Gasparini[a,b], U. Gasparini[a,b], S. Giorgetti[a], E. Lusiani[a], M. Margoni[a,b], A.T. Meneguzzo[a,b], M. Migliorini[a,b], J. Pazzini[a,b], P. Ronchese[a,b], R. Rossin[a,b], F. Simonetto[a,b], M. Tosi[a,b], A. Triossi[a,b], S. Ventura[a], M. Zanetti[a,b], P. Zotto[a,b], A. Zucchetta[a,b], G. Zumerle[a,b]

INFN Sezione di Pavia[a], Università di Pavia[b], Pavia, Italy
A. Braghieri[a], S. Calzaferri[a], D. Fiorina[a], P. Montagna[a,b], V. Re[a], C. Riccardi[a,b], P. Salvini[a], I. Vai[a,b], P. Vitulo[a,b]

INFN Sezione di Perugia[a], Università di Perugia[b], Perugia, Italy
S. Ajmal[a,b], M.E. Ascioti[a,b], G.M. Bilei[a], C. Carrivale[a,b], D. Ciangottini[a,b], L. Fanò[a,b], V. Mariani[a,b], M. Menichelli[a], F. Moscatelli[a,55], A. Rossi[a,b], A. Santocchia[a,b], D. Spiga[a], T. Tedeschi[a,b]

INFN Sezione di Pisa[a], Università di Pisa[b], Scuola Normale Superiore di Pisa[c], Pisa, Italy; Università di Siena[d], Siena, Italy
C. Aimè[a], C.A. Alexe[a,c], P. Asenov[a,b], P. Azzurri[a], G. Bagliesi[a], R. Bhattacharya[a], L. Bianchini[a,b], T. Boccali[a], E. Bossini[a], D. Bruschini[a,c], R. Castaldi[a], M.A. Ciocci[a,b], M. Cipriani[a,b], V. D'Amante[a,d], R. Dell'Orso[a], S. Donato[a,b], A. Giassi[a], F. Ligabue[a,c], A.C. Marini[a,b], D. Matos Figueiredo[a], A. Messineo[a,b], S. Mishra[a], V.K. Muraleedharan Nair Bindhu[a,b,42], M. Musich[a,b], S. Nandan[a], F. Palla[a], A. Rizzi[a,b],

JHEP01(2026)047

G. Rolandi[a,c], S. Roy Chowdhury[a], T. Sarkar[a], A. Scribano[a], P. Spagnolo[a], F. Tenchini[a,b], R. Tenchini[a], G. Tonelli[a,b], N. Turini[a,d], F. Vaselli[a,c], A. Venturi[a], P.G. Verdini[a]

INFN Sezione di Roma[a], Sapienza Università di Roma[b], Roma, Italy

P. Barria[a], C. Basile[a,b], F. Cavallari[a], L. Cunqueiro Mendez[a,b], D. Del Re[a,b], E. Di Marco[a,b], M. Diemoz[a], F. Errico[a,b], R. Gargiulo[a,b], E. Longo[a,b], L. Martikainen[a,b], J. Mijuskovic[a,b], G. Organtini[a,b], F. Pandolfi[a], R. Paramatti[a,b], C. Quaranta[a,b], S. Rahatlou[a,b], C. Rovelli[a], F. Santanastasio[a,b], L. Soffi[a], V. Vladimirov[a,b]

INFN Sezione di Torino[a], Università di Torino[b], Torino, Italy; Università del Piemonte Orientale[c], Novara, Italy

N. Amapane[a,b], R. Arcidiacono[a,c], S. Argiro[a,b], M. Arneodo[a,c], N. Bartosik[a], R. Bellan[a,b], C. Biino[a], C. Borca[a,b], N. Cartiglia[a], M. Costa[a,b], R. Covarelli[a,b], N. Demaria[a], L. Finco[a], M. Grippo[a,b], B. Kiani[a,b], F. Legger[a], F. Luongo[a,b], C. Mariotti[a], L. Markovic[a,b], S. Maselli[a], A. Mecca[a,b], L. Menzio[a,b], P. Meridiani[a], E. Migliore[a,b], M. Monteno[a], R. Mulargia[a], M.M. Obertino[a,b], G. Ortona[a], L. Pacher[a,b], N. Pastrone[a], M. Pelliccioni[a], M. Ruspa[a,c], F. Siviero[a,b], V. Sola[a,b], A. Solano[a,b], A. Staiano[a], C. Tarricone[a,b], D. Trocino[a], G. Umoret[a,b], R. White[a,b]

INFN Sezione di Trieste[a], Università di Trieste[b], Trieste, Italy

J. Babbar[a,b], S. Belforte[a], V. Candelise[a,b], M. Casarsa[a], F. Cossutti[a], K. De Leo[a], G. Della Ricca[a,b]

Kyungpook National University, Daegu, South Korea

S. Dogra, J. Hong, J. Kim, D. Lee, H. Lee, S.W. Lee, C.S. Moon, Y.D. Oh, M.S. Ryu, S. Sekmen, B. Tae, Y.C. Yang

Department of Mathematics and Physics - GWNU, Gangneung, South Korea

M.S. Kim

Chonnam National University, Institute for Universe and Elementary Particles, Kwangju, South Korea

G. Bak, P. Gwak, H. Kim, D.H. Moon

Hanyang University, Seoul, South Korea

E. Asilar, J. Choi[56], D. Kim, T.J. Kim, J.A. Merlin, Y. Ryou

Korea University, Seoul, South Korea

S. Choi, S. Han, B. Hong, K. Lee, K.S. Lee, S. Lee, J. Yoo

Kyung Hee University, Department of Physics, Seoul, South Korea

J. Goh, S. Yang

Sejong University, Seoul, South Korea

Y. Kang, H. S. Kim, Y. Kim, S. Lee

JHEP01(2026)047

Seoul National University, Seoul, South Korea
J. Almond, J.H. Bhyun, J. Choi, J. Choi, W. Jun, J. Kim, Y.W. Kim, S. Ko, H. Lee, J. Lee, J. Lee, B.H. Oh, S.B. Oh, H. Seo, U.K. Yang, I. Yoon

University of Seoul, Seoul, South Korea
W. Jang, D.Y. Kang, S. Kim, B. Ko, J.S.H. Lee, Y. Lee, I.C. Park, Y. Roh, I.J. Watson

Yonsei University, Department of Physics, Seoul, South Korea
S. Ha, K. Hwang, B. Kim, K. Lee, H.D. Yoo

Sungkyunkwan University, Suwon, South Korea
M. Choi, M.R. Kim, H. Lee, Y. Lee, I. Yu

College of Engineering and Technology, American University of the Middle East (AUM), Dasman, Kuwait
T. Beyrouthy, Y. Gharbia

Kuwait University - College of Science - Department of Physics, Safat, Kuwait
F. Alazemi

Riga Technical University, Riga, Latvia
K. Dreimanis, A. Gaile, C. Munoz Diaz, D. Osite, G. Pikurs, A. Potrebko, M. Seidel, D. Sidiropoulos Kontos

University of Latvia (LU), Riga, Latvia
N.R. Strautnieks

Vilnius University, Vilnius, Lithuania
M. Ambrozas, A. Juodagalvis, A. Rinkevicius, G. Tamulaitis

National Centre for Particle Physics, Universiti Malaya, Kuala Lumpur, Malaysia
I. Yusuff[57], Z. Zolkapli

Universidad de Sonora (UNISON), Hermosillo, Mexico
J.F. Benitez, A. Castaneda Hernandez, H.A. Encinas Acosta, L.G. Gallegos Maríñez, M. León Coello, J.A. Murillo Quijada, A. Sehrawat, L. Valencia Palomo

Centro de Investigacion y de Estudios Avanzados del IPN, Mexico City, Mexico
G. Ayala, H. Castilla-Valdez, H. Crotte Ledesma, E. De La Cruz-Burelo, I. Heredia-De La Cruz[58], R. Lopez-Fernandez, J. Mejia Guisao, A. Sánchez Hernández

Universidad Iberoamericana, Mexico City, Mexico
C. Oropeza Barrera, D.L. Ramirez Guadarrama, M. Ramírez García

Benemerita Universidad Autonoma de Puebla, Puebla, Mexico
I. Bautista, F.E. Neri Huerta, I. Pedraza, H.A. Salazar Ibarguen, C. Uribe Estrada

JHEP01(2026)047

University of Montenegro, Podgorica, Montenegro
I. Bubanja, N. Raicevic

University of Canterbury, Christchurch, New Zealand
P.H. Butler

National Centre for Physics, Quaid-I-Azam University, Islamabad, Pakistan
A. Ahmad, M.I. Asghar, A. Awais, M.I.M. Awan, H.R. Hoorani, W.A. Khan

AGH University of Krakow, Krakow, Poland
V. Avati, A. Bellora, L. Forthomme, L. Grzanka, M. Malawski, K. Piotrzkowski

National Centre for Nuclear Research, Swierk, Poland
H. Bialkowska, M. Bluj, M. Górski, M. Kazana, M. Szleper, P. Zalewski

Institute of Experimental Physics, Faculty of Physics, University of Warsaw, Warsaw, Poland
K. Bunkowski, K. Doroba, A. Kalinowski, M. Konecki, J. Krolikowski, A. Muhammad

Warsaw University of Technology, Warsaw, Poland
P. Fokow, K. Pozniak, W. Zabolotny

Laboratório de Instrumentação e Física Experimental de Partículas, Lisboa, Portugal
M. Araujo, D. Bastos, C. Beirão Da Cruz E Silva, A. Boletti, M. Bozzo, T. Camporesi, G. Da Molin, P. Faccioli, M. Gallinaro, J. Hollar, N. Leonardo, G.B. Marozzo, A. Petrilli, M. Pisano, J. Seixas, J. Varela, J.W. Wulff

Faculty of Physics, University of Belgrade, Belgrade, Serbia
P. Adzic, P. Milenovic

VINCA Institute of Nuclear Sciences, University of Belgrade, Belgrade, Serbia
D. Devetak, M. Dordevic, J. Milosevic, L. Nadderd, V. Rekovic, M. Stojanovic

Centro de Investigaciones Energéticas Medioambientales y Tecnológicas (CIEMAT), Madrid, Spain
J. Alcaraz Maestre, Cristina F. Bedoya, J.A. Brochero Cifuentes, Oliver M. Carretero, M. Cepeda, M. Cerrada, N. Colino, B. De La Cruz, A. Delgado Peris, A. Escalante Del Valle, D. Fernández Del Val, J.P. Fernández Ramos, J. Flix, M.C. Fouz, O. Gonzalez Lopez, S. Goy Lopez, J.M. Hernandez, M.I. Josa, J. Llorente Merino, C. Martin Perez, E. Martin Viscasillas, D. Moran, C. M. Morcillo Perez, Á. Navarro Tobar, C. Perez Dengra, A. Pérez-Calero Yzquierdo, J. Puerta Pelayo, I. Redondo, J. Sastre, J. Vazquez Escobar

Universidad Autónoma de Madrid, Madrid, Spain
J.F. de Trocóniz

JHEP01(2026)047

Universidad de Oviedo, Instituto Universitario de Ciencias y Tecnologías Espaciales de Asturias (ICTEA), Oviedo, Spain
B. Alvarez Gonzalez, J. Cuevas, J. Fernandez Menendez, S. Folgueras, I. Gonzalez Caballero, P. Leguina, E. Palencia Cortezon, J. Prado Pico, V. Rodríguez Bouza, A. Soto Rodríguez, A. Trapote, C. Vico Villalba, P. Vischia

Instituto de Física de Cantabria (IFCA), CSIC-Universidad de Cantabria, Santander, Spain
S. Blanco Fernández, I.J. Cabrillo, A. Calderon, J. Duarte Campderros, M. Fernandez, G. Gomez, C. Lasaosa García, R. Lopez Ruiz, C. Martinez Rivero, P. Martinez Ruiz del Arbol, F. Matorras, P. Matorras Cuevas, E. Navarrete Ramos, J. Piedra Gomez, L. Scodellaro, I. Vila, J.M. Vizan Garcia

University of Colombo, Colombo, Sri Lanka
B. Kailasapathy[59], D.D.C. Wickramarathna

University of Ruhuna, Department of Physics, Matara, Sri Lanka
W.G.D. Dharmaratna[60], K. Liyanage, N. Perera

CERN, European Organization for Nuclear Research, Geneva, Switzerland
D. Abbaneo, C. Amendola, E. Auffray, J. Baechler, D. Barney, A. Bermúdez Martínez, M. Bianco, A.A. Bin Anuar, A. Bocci, L. Borgonovi, C. Botta, A. Bragagnolo, E. Brondolin, C.E. Brown, C. Caillol, G. Cerminara, N. Chernyavskaya, D. d'Enterria, A. Dabrowski, A. David, A. De Roeck, M.M. Defranchis, M. Deile, M. Dobson, G. Franzoni, W. Funk, S. Giani, D. Gigi, K. Gill, F. Glege, M. Glowacki, J. Hegeman, J.K. Heikkilä, B. Huber, V. Innocente, T. James, P. Janot, O. Kaluzinska, O. Karacheban[29], G. Karathanasis, S. Laurila, P. Lecoq, E. Leutgeb, C. Lourenço, M. Magherini, L. Malgeri, M. Mannelli, M. Matthewman, A. Mehta, F. Meijers, S. Mersi, E. Meschi, V. Milosevic, F. Monti, F. Moortgat, M. Mulders, I. Neutelings, S. Orfanelli, F. Pantaleo, G. Petrucciani, A. Pfeiffer, M. Pierini, M. Pitt, H. Qu, D. Rabady, B. Ribeiro Lopes, F. Riti, M. Rovere, H. Sakulin, R. Salvatico, S. Sanchez Cruz, S. Scarfi, C. Schwick, M. Selvaggi, A. Sharma, K. Shchelina, P. Silva, P. Sphicas[61], A.G. Stahl Leiton, A. Steen, S. Summers, D. Treille, P. Tropea, D. Walter, J. Wanczyk[62], J. Wang, S. Wuchterl, P. Zehetner, P. Zejdl, W.D. Zeuner

PSI Center for Neutron and Muon Sciences, Villigen, Switzerland
T. Bevilacqua[63], L. Caminada[63], A. Ebrahimi, W. Erdmann, R. Horisberger, Q. Ingram, H.C. Kaestli, D. Kotlinski, C. Lange, M. Missiroli[63], L. Noehte[63], T. Rohe, A. Samalan

ETH Zurich - Institute for Particle Physics and Astrophysics (IPA), Zurich, Switzerland
T.K. Aarrestad, M. Backhaus, G. Bonomelli, A. Calandri, C. Cazzaniga, K. Datta, P. De Bryas Dexmiers D'archiac[62], A. De Cosa, G. Dissertori, M. Dittmar, M. Donegà, F. Eble, M. Galli, K. Gedia, F. Glessgen, C. Grab, N. Härringer, T.G. Harte, D. Hits, W. Lustermann, A.-M. Lyon, R.A. Manzoni, M. Marchegiani, L. Marchese,

A. Mascellani[62], F. Nessi-Tedaldi, F. Pauss, V. Perovic, S. Pigazzini, B. Ristic, R. Seidita, J. Steggemann[62], A. Tarabini, D. Valsecchi, R. Wallny

Universität Zürich, Zurich, Switzerland
C. Amsler[64], P. Bärtschi, M.F. Canelli, K. Cormier, M. Huwiler, W. Jin, A. Jofrehei, B. Kilminster, S. Leontsinis, S.P. Liechti, A. Macchiolo, P. Meiring, F. Meng, J. Motta, A. Reimers, P. Robmann, M. Senger, E. Shokr, F. Stäger, R. Tramontano

National Central University, Chung-Li, Taiwan
C. Adloff[65], D. Bhowmik, C.M. Kuo, W. Lin, P.K. Rout, P.C. Tiwari[39]

National Taiwan University (NTU), Taipei, Taiwan
L. Ceard, K.F. Chen, Z.g. Chen, A. De Iorio, W.-S. Hou, T.h. Hsu, Y.w. Kao, S. Karmakar, G. Kole, Y.y. Li, R.-S. Lu, E. Paganis, X.f. Su, J. Thomas-Wilsker, L.s. Tsai, D. Tsionou, H.y. Wu, E. Yazgan

High Energy Physics Research Unit, Department of Physics, Faculty of Science, Chulalongkorn University, Bangkok, Thailand
C. Asawatangtrakuldee, N. Srimanobhas, V. Wachirapusitanand

Tunis El Manar University, Tunis, Tunisia
Y. Maghrbi

Çukurova University, Physics Department, Science and Art Faculty, Adana, Turkey
D. Agyel, F. Boran, F. Dolek, I. Dumanoglu[66], E. Eskut, Y. Guler[67], E. Gurpinar Guler[67], C. Isik, O. Kara, A. Kayis Topaksu, Y. Komurcu, G. Onengut, K. Ozdemir[68], A. Polatoz, B. Tali[69], U.G. Tok, E. Uslan, I.S. Zorbakir

Middle East Technical University, Physics Department, Ankara, Turkey
M. Yalvac[70]

Bogazici University, Istanbul, Turkey
B. Akgun, I.O. Atakisi, E. Gülmez, M. Kaya[71], O. Kaya[72], S. Tekten[73]

Istanbul Technical University, Istanbul, Turkey
A. Cakir, K. Cankocak[66,74], S. Sen[75]

Istanbul University, Istanbul, Turkey
O. Aydilek[76], B. Hacisahinoglu, I. Hos[77], B. Kaynak, S. Ozkorucuklu, O. Potok, H. Sert, C. Simsek, C. Zorbilmez

Yildiz Technical University, Istanbul, Turkey
S. Cerci, B. Isildak[78], D. Sunar Cerci, T. Yetkin

Institute for Scintillation Materials of National Academy of Science of Ukraine, Kharkiv, Ukraine
A. Boyaryntsev, B. Grynyov

JHEP01(2026)047

National Science Centre, Kharkiv Institute of Physics and Technology, Kharkiv, Ukraine
L. Levchuk

University of Bristol, Bristol, U.K.
D. Anthony, J.J. Brooke, A. Bundock, F. Bury, E. Clement, D. Cussans, H. Flacher, J. Goldstein, H.F. Heath, M.-L. Holmberg, L. Kreczko, S. Paramesvaran, L. Robertshaw, V.J. Smith, K. Walkingshaw Pass

Rutherford Appleton Laboratory, Didcot, U.K.
A.H. Ball, K.W. Bell, A. Belyaev[79], C. Brew, R.M. Brown, D.J.A. Cockerill, C. Cooke, A. Elliot, K.V. Ellis, K. Harder, S. Harper, J. Linacre, K. Manolopoulos, D.M. Newbold, E. Olaiya, D. Petyt, T. Reis, A.R. Sahasransu, G. Salvi, T. Schuh, C.H. Shepherd-Themistocleous, I.R. Tomalin, K.C. Whalen, T. Williams

Imperial College, London, U.K.
I. Andreou, R. Bainbridge, P. Bloch, O. Buchmuller, C.A. Carrillo Montoya, G.S. Chahal[80], D. Colling, J.S. Dancu, I. Das, P. Dauncey, G. Davies, M. Della Negra, S. Fayer, G. Fedi, G. Hall, A. Howard, G. Iles, C.R. Knight, P. Krueper, J. Langford, K.H. Law, J. León Holgado, L. Lyons, A.-M. Magnan, B. Maier, S. Mallios, M. Mieskolainen, J. Nash[81], M. Pesaresi, P.B. Pradeep, B.C. Radburn-Smith, A. Richards, A. Rose, K. Savva, C. Seez, R. Shukla, A. Tapper, K. Uchida, G.P. Uttley, T. Virdee[31], M. Vojinovic, N. Wardle, D. Winterbottom

Brunel University, Uxbridge, U.K.
J.E. Cole, A. Khan, P. Kyberd, I.D. Reid

Baylor University, Waco, Texas, U.S.A.
S. Abdullin, A. Brinkerhoff, E. Collins, M.R. Darwish, J. Dittmann, K. Hatakeyama, V. Hegde, J. Hiltbrand, B. McMaster, J. Samudio, S. Sawant, C. Sutantawibul, J. Wilson

Catholic University of America, Washington, DC, U.S.A.
R. Bartek, A. Dominguez, A.E. Simsek, S.S. Yu

The University of Alabama, Tuscaloosa, Alabama, U.S.A.
B. Bam, A. Buchot Perraguin, R. Chudasama, S.I. Cooper, C. Crovella, S.V. Gleyzer, E. Pearson, C.U. Perez, P. Rumerio[82], E. Usai, R. Yi

Boston University, Boston, Massachusetts, U.S.A.
A. Akpinar, C. Cosby, G. De Castro, Z. Demiragli, C. Erice, C. Fangmeier, C. Fernandez Madrazo, E. Fontanesi, D. Gastler, F. Golf, S. Jeon, J. O'cain, I. Reed, J. Rohlf, K. Salyer, D. Sperka, D. Spitzbart, I. Suarez, A. Tsatsos, A.G. Zecchinelli

JHEP01(2026)047

Brown University, Providence, Rhode Island, U.S.A.
G. Barone, G. Benelli, D. Cutts, S. Ellis, L. Gouskos, M. Hadley, U. Heintz, K.W. Ho, J.M. Hogan[83], T. Kwon, G. Landsberg, K.T. Lau, J. Luo, S. Mondal, T. Russell, S. Sagir[84], X. Shen, M. Stamenkovic, N. Venkatasubramanian

University of California, Davis, Davis, California, U.S.A.
S. Abbott, B. Barton, C. Brainerd, R. Breedon, H. Cai, M. Calderon De La Barca Sanchez, M. Chertok, M. Citron, J. Conway, P.T. Cox, R. Erbacher, F. Jensen, O. Kukral, G. Mocellin, M. Mulhearn, S. Ostrom, W. Wei, S. Yoo, F. Zhang

University of California, Los Angeles, California, U.S.A.
K. Adamidis, M. Bachtis, D. Campos, R. Cousins, A. Datta, G. Flores Avila, J. Hauser, M. Ignatenko, M.A. Iqbal, T. Lam, Y.f. Lo, E. Manca, A. Nunez Del Prado, D. Saltzberg, V. Valuev

University of California, Riverside, Riverside, California, U.S.A.
R. Clare, J.W. Gary, G. Hanson

University of California, San Diego, La Jolla, California, U.S.A.
A. Aportela, A. Arora, J.G. Branson, S. Cittolin, S. Cooperstein, D. Diaz, J. Duarte, L. Giannini, Y. Gu, J. Guiang, R. Kansal, V. Krutelyov, R. Lee, J. Letts, M. Masciovecchio, F. Mokhtar, S. Mukherjee, M. Pieri, D. Primosch, M. Quinnan, V. Sharma, M. Tadel, E. Vourliotis, F. Würthwein, Y. Xiang, A. Yagil

University of California, Santa Barbara - Department of Physics, Santa Barbara, California, U.S.A.
A. Barzdukas, L. Brennan, C. Campagnari, K. Downham, C. Grieco, M.M. Hussain, J. Incandela, J. Kim, A.J. Li, P. Masterson, H. Mei, J. Richman, S.N. Santpur, U. Sarica, R. Schmitz, F. Setti, J. Sheplock, D. Stuart, T.Á. Vámi, X. Yan, D. Zhang

California Institute of Technology, Pasadena, California, U.S.A.
S. Bhattacharya, A. Bornheim, O. Cerri, J. Mao, H.B. Newman, G. Reales Gutiérrez, M. Spiropulu, J.R. Vlimant, C. Wang, S. Xie, R.Y. Zhu

Carnegie Mellon University, Pittsburgh, Pennsylvania, U.S.A.
J. Alison, S. An, P. Bryant, M. Cremonesi, V. Dutta, T. Ferguson, T.A. Gómez Espinosa, A. Harilal, A. Kallil Tharayil, M. Kanemura, C. Liu, T. Mudholkar, S. Murthy, P. Palit, K. Park, M. Paulini, A. Roberts, A. Sanchez, W. Terrill

University of Colorado Boulder, Boulder, Colorado, U.S.A.
J.P. Cumalat, W.T. Ford, A. Hart, A. Hassani, N. Manganelli, J. Pearkes, C. Savard, N. Schonbeck, K. Stenson, K.A. Ulmer, S.R. Wagner, N. Zipper, D. Zuolo

JHEP01(2026)047

Cornell University, Ithaca, New York, U.S.A.
J. Alexander, X. Chen, D.J. Cranshaw, J. Dickinson, J. Fan, X. Fan, S. Hogan, P. Kotamnives, J. Monroy, M. Oshiro, J.R. Patterson, M. Reid, A. Ryd, J. Thom, P. Wittich, R. Zou

Fermi National Accelerator Laboratory, Batavia, Illinois, U.S.A.
M. Albrow, M. Alyari, O. Amram, G. Apollinari, A. Apresyan, L.A.T. Bauerdick, D. Berry, J. Berryhill, P.C. Bhat, K. Burkett, J.N. Butler, A. Canepa, G.B. Cerati, H.W.K. Cheung, F. Chlebana, G. Cummings, I. Dutta, V.D. Elvira, J. Freeman, A. Gandrakota, Z. Gecse, L. Gray, D. Green, A. Grummer, S. Grünendahl, D. Guerrero, O. Gutsche, R.M. Harris, T.C. Herwig, J. Hirschauer, B. Jayatilaka, S. Jindariani, M. Johnson, U. Joshi, T. Klijnsma, B. Klima, K.H.M. Kwok, S. Lammel, C. Lee, D. Lincoln, R. Lipton, T. Liu, K. Maeshima, D. Mason, P. McBride, P. Merkel, S. Mrenna, S. Nahn, J. Ngadiuba, D. Noonan, S. Norberg, V. Papadimitriou, N. Pastika, K. Pedro, C. Pena[85], F. Ravera, A. Reinsvold Hall[86], L. Ristori, M. Safdari, E. Sexton-Kennedy, N. Smith, A. Soha, L. Spiegel, S. Stoynev, J. Strait, L. Taylor, S. Tkaczyk, N.V. Tran, L. Uplegger, E.W. Vaandering, I. Zoi

University of Florida, Gainesville, Florida, U.S.A.
C. Aruta, P. Avery, D. Bourilkov, P. Chang, V. Cherepanov, R.D. Field, C. Huh, E. Koenig, M. Kolosova, J. Konigsberg, A. Korytov, K. Matchev, N. Menendez, G. Mitselmakher, K. Mohrman, A. Muthirakalayil Madhu, N. Rawal, S. Rosenzweig, Y. Takahashi, J. Wang

Florida State University, Tallahassee, Florida, U.S.A.
T. Adams, A. Al Kadhim, A. Askew, S. Bower, R. Hashmi, R.S. Kim, S. Kim, T. Kolberg, G. Martinez, H. Prosper, P.R. Prova, M. Wulansatiti, R. Yohay, J. Zhang

Florida Institute of Technology, Melbourne, Florida, U.S.A.
B. Alsufyani, S. Butalla, S. Das, T. Elkafrawy[87], M. Hohlmann, E. Yanes

University of Illinois Chicago, Chicago, Illinois, U.S.A.
M.R. Adams, A. Baty, C. Bennett, R. Cavanaugh, R. Escobar Franco, O. Evdokimov, C.E. Gerber, M. Hawksworth, A. Hingrajiya, D.J. Hofman, J.h. Lee, D. S. Lemos, C. Mills, S. Nanda, G. Oh, B. Ozek, D. Pilipovic, R. Pradhan, E. Prifti, P. Roy, T. Roy, S. Rudrabhatla, N. Singh, M.B. Tonjes, N. Varelas, M.A. Wadud, Z. Ye, J. Yoo

The University of Iowa, Iowa City, Iowa, U.S.A.
M. Alhusseini, D. Blend, K. Dilsiz[88], L. Emediato, G. Karaman, O.K. Köseyan, J.-P. Merlo, A. Mestvirishvili[89], O. Neogi, H. Ogul[90], Y. Onel, A. Penzo, C. Snyder, E. Tiras[91]

Johns Hopkins University, Baltimore, Maryland, U.S.A.
B. Blumenfeld, L. Corcodilos, J. Davis, A.V. Gritsan, L. Kang, S. Kyriacou, P. Maksimovic, M. Roguljic, J. Roskes, S. Sekhar, M. Swartz

JHEP01(2026)047

The University of Kansas, Lawrence, Kansas, U.S.A.
A. Abreu, L.F. Alcerro Alcerro, J. Anguiano, S. Arteaga Escatel, P. Baringer, A. Bean, Z. Flowers, D. Grove, J. King, G. Krintiras, M. Lazarovits, C. Le Mahieu, J. Marquez, M. Murray, M. Nickel, S. Popescu[92], C. Rogan, C. Royon, S. Sanders, C. Smith, G. Wilson

Kansas State University, Manhattan, Kansas, U.S.A.
B. Allmond, R. Gujju Gurunadha, A. Ivanov, K. Kaadze, Y. Maravin, J. Natoli, D. Roy, G. Sorrentino

University of Maryland, College Park, Maryland, U.S.A.
A. Baden, A. Belloni, J. Bistany-riebman, Y.M. Chen, S.C. Eno, N.J. Hadley, S. Jabeen, R.G. Kellogg, T. Koeth, B. Kronheim, S. Lascio, A.C. Mignerey, S. Nabili, C. Palmer, C. Papageorgakis, M.M. Paranjpe, E. Popova[93], A. Shevelev, L. Wang, L. Zhang

Massachusetts Institute of Technology, Cambridge, Massachusetts, U.S.A.
C. Baldenegro Barrera, J. Bendavid, S. Bright-Thonney, I.A. Cali, P.c. Chou, M. D'Alfonso, J. Eysermans, C. Freer, G. Gomez-Ceballos, M. Goncharov, G. Grosso, P. Harris, D. Hoang, D. Kovalskyi, J. Krupa, L. Lavezzo, Y.-J. Lee, K. Long, C. Mcginn, A. Novak, M.I. Park, C. Paus, C. Reissel, C. Roland, G. Roland, S. Rothman, G.S.F. Stephans, Z. Wang, B. Wyslouch, T. J. Yang

University of Minnesota, Minneapolis, Minnesota, U.S.A.
B. Crossman, C. Kapsiak, M. Krohn, D. Mahon, J. Mans, B. Marzocchi, M. Revering, R. Rusack, R. Saradhy, N. Strobbe

University of Nebraska-Lincoln, Lincoln, Nebraska, U.S.A.
K. Bloom, D.R. Claes, G. Haza, J. Hossain, C. Joo, I. Kravchenko, A. Rohilla, J.E. Siado, W. Tabb, A. Vagnerini, A. Wightman, F. Yan, D. Yu

State University of New York at Buffalo, Buffalo, New York, U.S.A.
H. Bandyopadhyay, L. Hay, H.w. Hsia, I. Iashvili, A. Kalogeropoulos, A. Kharchilava, M. Morris, D. Nguyen, S. Rappoccio, H. Rejeb Sfar, A. Williams, P. Young

Northeastern University, Boston, Massachusetts, U.S.A.
G. Alverson, E. Barberis, J. Bonilla, B. Bylsma, M. Campana, J. Dervan, Y. Haddad, Y. Han, I. Israr, A. Krishna, P. Levchenko, J. Li, M. Lu, R. Mccarthy, D.M. Morse, T. Orimoto, A. Parker, L. Skinnari, E. Tsai, D. Wood

Northwestern University, Evanston, Illinois, U.S.A.
S. Dittmer, K.A. Hahn, D. Li, Y. Liu, M. Mcginnis, Y. Miao, D.G. Monk, M.H. Schmitt, A. Taliercio, M. Velasco

University of Notre Dame, Notre Dame, Indiana, U.S.A.
G. Agarwal, R. Band, R. Bucci, S. Castells, A. Das, R. Goldouzian, M. Hildreth, K. Hurtado Anampa, T. Ivanov, C. Jessop, K. Lannon, J. Lawrence, N. Loukas,

L. Lutton, J. Mariano, N. Marinelli, I. Mcalister, T. McCauley, C. Mcgrady, C. Moore, Y. Musienko[24], H. Nelson, M. Osherson, A. Piccinelli, R. Ruchti, A. Townsend, Y. Wan, M. Wayne, H. Yockey, M. Zarucki, L. Zygala

The Ohio State University, Columbus, Ohio, U.S.A.
A. Basnet, M. Carrigan, L.S. Durkin, C. Hill, M. Joyce, M. Nunez Ornelas, K. Wei, D.A. Wenzl, B.L. Winer, B. R. Yates

Princeton University, Princeton, New Jersey, U.S.A.
H. Bouchamaoui, K. Coldham, P. Das, G. Dezoort, P. Elmer, P. Fackeldey, A. Frankenthal, B. Greenberg, N. Haubrich, K. Kennedy, G. Kopp, S. Kwan, Y. Lai, D. Lange, A. Loeliger, D. Marlow, I. Ojalvo, J. Olsen, F. Simpson, D. Stickland, C. Tully, L.H. Vage

University of Puerto Rico, Mayaguez, Puerto Rico, U.S.A.
S. Malik, R. Sharma

Purdue University, West Lafayette, Indiana, U.S.A.
A.S. Bakshi, S. Chandra, R. Chawla, A. Gu, L. Gutay, M. Jones, A.W. Jung, A.M. Koshy, M. Liu, G. Negro, N. Neumeister, G. Paspalaki, S. Piperov, J.F. Schulte, A. K. Virdi, F. Wang, A. Wildridge, W. Xie, Y. Yao

Purdue University Northwest, Hammond, Indiana, U.S.A.
J. Dolen, N. Parashar, A. Pathak

Rice University, Houston, Texas, U.S.A.
D. Acosta, A. Agrawal, T. Carnahan, K.M. Ecklund, P.J. Fernández Manteca, S. Freed, P. Gardner, F.J.M. Geurts, I. Krommydas, W. Li, J. Lin, O. Miguel Colin, B.P. Padley, R. Redjimi, J. Rotter, E. Yigitbasi, Y. Zhang

University of Rochester, Rochester, New York, U.S.A.
A. Bodek, P. de Barbaro, R. Demina, J.L. Dulemba, A. Garcia-Bellido, O. Hindrichs, A. Khukhunaishvili, N. Parmar, P. Parygin[93], R. Taus

Rutgers, The State University of New Jersey, Piscataway, New Jersey, U.S.A.
B. Chiarito, J.P. Chou, S.V. Clark, D. Gadkari, Y. Gershtein, E. Halkiadakis, M. Heindl, C. Houghton, D. Jaroslawski, S. Konstantinou, I. Laflotte, A. Lath, R. Montalvo, K. Nash, J. Reichert, P. Saha, S. Salur, S. Schnetzer, S. Somalwar, R. Stone, S.A. Thayil, S. Thomas, J. Vora

University of Tennessee, Knoxville, Tennessee, U.S.A.
D. Ally, A.G. Delannoy, S. Fiorendi, S. Higginbotham, T. Holmes, A.R. Kanuganti, N. Karunarathna, L. Lee, E. Nibigira, S. Spanier

Texas A&M University, College Station, Texas, U.S.A.
D. Aebi, M. Ahmad, T. Akhter, K. Androsov[62], O. Bouhali[94], R. Eusebi, J. Gilmore, T. Huang, T. Kamon[95], H. Kim, S. Luo, R. Mueller, D. Overton, A. Safonov

Texas Tech University, Lubbock, Texas, U.S.A.
N. Akchurin, J. Damgov, Y. Feng, N. Gogate, Y. Kazhykarim, K. Lamichhane, S.W. Lee, C. Madrid, A. Mankel, T. Peltola, I. Volobouev

Vanderbilt University, Nashville, Tennessee, U.S.A.
E. Appelt, Y. Chen, S. Greene, A. Gurrola, W. Johns, R. Kunnawalkam Elayavalli, A. Melo, D. Rathjens, F. Romeo, P. Sheldon, S. Tuo, J. Velkovska, J. Viinikainen

University of Virginia, Charlottesville, Virginia, U.S.A.
B. Cardwell, H. Chung, B. Cox, J. Hakala, R. Hirosky, A. Ledovskoy, C. Mantilla, C. Neu, C. Ramón Álvarez

Wayne State University, Detroit, Michigan, U.S.A.
S. Bhattacharya, P.E. Karchin

University of Wisconsin - Madison, Madison, Wisconsin, U.S.A.
A. Aravind, S. Banerjee, K. Black, T. Bose, E. Chavez, S. Dasu, P. Everaerts, C. Galloni, H. He, M. Herndon, A. Herve, C.K. Koraka, A. Lanaro, R. Loveless, J. Madhusudanan Sreekala, A. Mallampalli, A. Mohammadi, S. Mondal, G. Parida, L. Pétré, D. Pinna, A. Savin, V. Shang, V. Sharma, W.H. Smith, D. Teague, H.F. Tsoi, W. Vetens, A. Warden

Authors affiliated with an international laboratory covered by a cooperation agreement with CERN
S. Afanasiev, V. Alexakhin, D. Budkouski, I. Golutvin[†], I. Gorbunov, V. Karjavine, O. Kodolova[96,93], V. Korenkov, A. Lanev, A. Malakhov, V. Matveev[97], A. Nikitenko[98,96], V. Palichik, V. Perelygin, M. Savina, V. Shalaev, S. Shmatov, S. Shulha, V. Smirnov, O. Teryaev, N. Voytishin, B.S. Yuldashev[†,99], A. Zarubin, I. Zhizhin, Yu. Andreev, A. Dermenev, S. Gninenko, N. Golubev, A. Karneyeu, D. Kirpichnikov, M. Kirsanov, N. Krasnikov, I. Tlisova, A. Toropin

Authors affiliated with an institute formerly covered by a cooperation agreement with CERN
G. Gavrilov, V. Golovtcov, Y. Ivanov, V. Kim[100], V. Murzin, V. Oreshkin, D. Sosnov, V. Sulimov, L. Uvarov, A. Vorobyev[†], T. Aushev, K. Ivanov, V. Gavrilov, N. Lychkovskaya, V. Popov, A. Zhokin, M. Chadeeva[100], R. Chistov[100], S. Polikarpov[100], V. Andreev, M. Azarkin, M. Kirakosyan, A. Terkulov, E. Boos, V. Bunichev, M. Dubinin[85], L. Dudko, V. Klyukhin, O. Lukina, M. Perfilov, V. Savrin, A. Snigirev, G. Vorotnikov, V. Blinov[100], T. Dimova[100], A. Kozyrev[100], O. Radchenko[100], Y. Skovpen[100], V. Kachanov, S. Slabospitskii, A. Uzunian, A. Babaev, V. Borshch, D. Druzhkin

[†] *Deceased*
[1] *Also at Yerevan State University, Yerevan, Armenia*
[2] *Also at TU Wien, Vienna, Austria*
[3] *Also at Ghent University, Ghent, Belgium*

JHEP01(2026)047

[4] *Also at Universidade do Estado do Rio de Janeiro, Rio de Janeiro, Brazil*
[5] *Also at FACAMP - Faculdades de Campinas, Sao Paulo, Brazil*
[6] *Also at Universidade Estadual de Campinas, Campinas, Brazil*
[7] *Also at Federal University of Rio Grande do Sul, Porto Alegre, Brazil*
[8] *Also at University of Chinese Academy of Sciences, Beijing, China*
[9] *Also at China Center of Advanced Science and Technology, Beijing, China*
[10] *Also at University of Chinese Academy of Sciences, Beijing, China*
[11] *Also at China Spallation Neutron Source, Guangdong, China*
[12] *Now at Henan Normal University, Xinxiang, China*
[13] *Also at University of Shanghai for Science and Technology, Shanghai, China*
[14] *Now at The University of Iowa, Iowa City, Iowa, U.S.A.*
[15] *Also at an institute formerly covered by a cooperation agreement with CERN*
[16] *Also at Helwan University, Cairo, Egypt*
[17] *Now at Zewail City of Science and Technology, Zewail, Egypt*
[18] *Now at British University in Egypt, Cairo, Egypt*
[19] *Now at Cairo University, Cairo, Egypt*
[20] *Also at Purdue University, West Lafayette, Indiana, U.S.A.*
[21] *Also at Université de Haute Alsace, Mulhouse, France*
[22] *Also at Istinye University, Istanbul, Turkey*
[23] *Also at Tbilisi State University, Tbilisi, Georgia*
[24] *Also at an international laboratory covered by a cooperation agreement with CERN*
[25] *Also at The University of the State of Amazonas, Manaus, Brazil*
[26] *Also at University of Hamburg, Hamburg, Germany*
[27] *Also at RWTH Aachen University, III. Physikalisches Institut A, Aachen, Germany*
[28] *Also at Bergische University Wuppertal (BUW), Wuppertal, Germany*
[29] *Also at Brandenburg University of Technology, Cottbus, Germany*
[30] *Also at Forschungszentrum Jülich, Juelich, Germany*
[31] *Also at CERN, European Organization for Nuclear Research, Geneva, Switzerland*
[32] *Also at HUN-REN ATOMKI - Institute of Nuclear Research, Debrecen, Hungary*
[33] *Now at Universitatea Babes-Bolyai - Facultatea de Fizica, Cluj-Napoca, Romania*
[34] *Also at MTA-ELTE Lendület CMS Particle and Nuclear Physics Group, Eötvös Loránd University, Budapest, Hungary*
[35] *Also at HUN-REN Wigner Research Centre for Physics, Budapest, Hungary*
[36] *Also at Physics Department, Faculty of Science, Assiut University, Assiut, Egypt*
[37] *Also at Punjab Agricultural University, Ludhiana, India*
[38] *Also at University of Visva-Bharati, Santiniketan, India*
[39] *Also at Indian Institute of Science (IISc), Bangalore, India*
[40] *Also at Amity University Uttar Pradesh, Noida, India*
[41] *Also at IIT Bhubaneswar, Bhubaneswar, India*
[42] *Also at Institute of Physics, Bhubaneswar, India*
[43] *Also at University of Hyderabad, Hyderabad, India*
[44] *Also at Deutsches Elektronen-Synchrotron, Hamburg, Germany*
[45] *Also at Isfahan University of Technology, Isfahan, Iran*
[46] *Also at Sharif University of Technology, Tehran, Iran*
[47] *Also at Department of Physics, University of Science and Technology of Mazandaran, Behshahr, Iran*
[48] *Also at Department of Physics, Faculty of Science, Arak University, ARAK, Iran*
[49] *Also at Italian National Agency for New Technologies, Energy and Sustainable Economic Development, Bologna, Italy*
[50] *Also at Centro Siciliano di Fisica Nucleare e di Struttura Della Materia, Catania, Italy*
[51] *Also at Università degli Studi Guglielmo Marconi, Roma, Italy*
[52] *Also at Scuola Superiore Meridionale, Università di Napoli 'Federico II', Napoli, Italy*
[53] *Also at Fermi National Accelerator Laboratory, Batavia, Illinois, U.S.A.*
[54] *Also at Lulea University of Technology, Lulea, Sweden*

JHEP01(2026)047

[55] *Also at Consiglio Nazionale delle Ricerche - Istituto Officina dei Materiali, Perugia, Italy*
[56] *Also at Institut de Physique des 2 Infinis de Lyon (IP2I), Villeurbanne, France*
[57] *Also at Department of Applied Physics, Faculty of Science and Technology, Universiti Kebangsaan Malaysia, Bangi, Malaysia*
[58] *Also at Consejo Nacional de Ciencia y Tecnología, Mexico City, Mexico*
[59] *Also at Trincomalee Campus, Eastern University, Sri Lanka, Nilaveli, Sri Lanka*
[60] *Also at Saegis Campus, Nugegoda, Sri Lanka*
[61] *Also at National and Kapodistrian University of Athens, Athens, Greece*
[62] *Also at Ecole Polytechnique Fédérale Lausanne, Lausanne, Switzerland*
[63] *Also at Universität Zürich, Zurich, Switzerland*
[64] *Also at Stefan Meyer Institute for Subatomic Physics, Vienna, Austria*
[65] *Also at Laboratoire d'Annecy-le-Vieux de Physique des Particules, IN2P3-CNRS, Annecy-le-Vieux, France*
[66] *Also at Near East University, Research Center of Experimental Health Science, Mersin, Turkey*
[67] *Also at Konya Technical University, Konya, Turkey*
[68] *Also at Izmir Bakircay University, Izmir, Turkey*
[69] *Also at Adiyaman University, Adiyaman, Turkey*
[70] *Also at Bozok Universitetesi Rektörlügü, Yozgat, Turkey*
[71] *Also at Marmara University, Istanbul, Turkey*
[72] *Also at Milli Savunma University, Istanbul, Turkey*
[73] *Also at Kafkas University, Kars, Turkey*
[74] *Now at Istanbul Okan University, Istanbul, Turkey*
[75] *Also at Hacettepe University, Ankara, Turkey*
[76] *Also at Erzincan Binali Yildirim University, Erzincan, Turkey*
[77] *Also at Istanbul University - Cerrahpasa, Faculty of Engineering, Istanbul, Turkey*
[78] *Also at Yildiz Technical University, Istanbul, Turkey*
[79] *Also at School of Physics and Astronomy, University of Southampton, Southampton, U.K.*
[80] *Also at IPPP Durham University, Durham, U.K.*
[81] *Also at Monash University, Faculty of Science, Clayton, Australia*
[82] *Also at Università di Torino, Torino, Italy*
[83] *Also at Bethel University, St. Paul, Minnesota, U.S.A.*
[84] *Also at Karamanoğlu Mehmetbey University, Karaman, Turkey*
[85] *Also at California Institute of Technology, Pasadena, California, U.S.A.*
[86] *Also at United States Naval Academy, Annapolis, Maryland, U.S.A.*
[87] *Also at Ain Shams University, Cairo, Egypt*
[88] *Also at Bingol University, Bingol, Turkey*
[89] *Also at Georgian Technical University, Tbilisi, Georgia*
[90] *Also at Sinop University, Sinop, Turkey*
[91] *Also at Erciyes University, Kayseri, Turkey*
[92] *Also at Horia Hulubei National Institute of Physics and Nuclear Engineering (IFIN-HH), Bucharest, Romania*
[93] *Now at another institute formerly covered by a cooperation agreement with CERN*
[94] *Also at Texas A&M University at Qatar, Doha, Qatar*
[95] *Also at Kyungpook National University, Daegu, South Korea*
[96] *Also at Yerevan Physics Institute, Yerevan, Armenia*
[97] *Also at another international laboratory covered by a cooperation agreement with CERN*
[98] *Also at Imperial College, London, U.K.*
[99] *Also at Institute of Nuclear Physics of the Uzbekistan Academy of Sciences, Tashkent, Uzbekistan*
[100] *Also at another institute formerly covered by a cooperation agreement with CERN*

JHEP01(2026)047